Distribution Agreement

In presenting this thesis as a partial fulfillment of the requirements for a degree from Emory University, I hereby grant to Emory University and its agents the non-exclusive license to archive, make accessible, and display my thesis in whole or in part in all forms of media, now or hereafter now, including display on the World Wide Web. I understand that I may select some access restrictions as part of the online submission of this thesis. I retain all ownership rights to the copyright of the thesis. I also retain the right to use in future works (such as articles or books) all or part of this thesis.

Seth Young April 4, 2021

Controlling Biopolymer Phase Networks with Dynamic Chemical Networks

by

Seth Young

Dr. David Lynn

Adviser

Department of Chemistry

Dr. David Lynn

Adviser

Dr. Antonio Brathwaite

Committee Member

Dr. Kathleen Campbell

Committee Member

2021

Controlling Biopolymer Phase Networks with Dynamic Chemical Networks

By

Seth Young

Dr. David Lynn
Adviser

An abstract of
a thesis submitted to the Faculty of Emory College of Arts and Sciences
of Emory University in partial fulfillment
of the requirements of the degree of
Bachelor of Science with Honors

Department of Chemistry

2021

Abstract

Controlling Biopolymer Phase Networks with Dynamic Chemical Networks

By Seth Young

Collagen is a phenomenally versatile and dynamic structure necessary for the survival of almost all multicellular life. This protein's strong intermolecular forces provide physical support while remaining flexible through interspaced flexible elements. Multitudes of approaches have been taken to try and replicate the physical properties of this protein; however, most approaches have failed to capture the flexibility of collagen by solely focusing on developing a strong material without accounting for its dynamics. Utilizing the metastable pyrimidinone chemistry built by Chen et al., we set out to replicate the flexibility of collagen using a C-terminal aldehyde peptide asparagine proline glycine (NPG). This peptide successfully assembles into a fibrillar structure that bundles and eventually twists into a new structure termed 'ball of yarn.' In addition, this peptide was found to decrease apoptosis and increase differentiation of neurons in preliminary studies on brain organoids. Synthesis of this was then optimized and adapted to allow for a more expansive synthetic approach to C-terminal aldehyde peptides.

Controlling Biopolymer Phase Networks with Dynamic Chemical Networks

By

Seth Young

Dr. David Lynn

Adviser

A thesis submitted to the Faculty of Emory College of Arts and Sciences
of Emory University in partial fulfillment
of the requirements of the degree of
Bachelor of Science with Honors

Department of Chemistry

2021

Acknowledgements

First, I would like to acknowledge and thank my adviser Dr. Lynn. He took me in my freshman year and allowed me the space and guidance to develop as a scientist.

Second, I would like to acknowledge the graduate students of the Lynn lab for assisting me throughout my experiments. I especially want to acknowledge Christella and Youngsun for supporting me through many attempts in experiments and helping me at every opportunity. Without them, I would not have been able to complete this thesis.

Third, I would like to acknowledge my partner Vanessa for helping to support me through this project and providing her input through her immaculate organizational skills. I would have not come even a fraction as far as I have without you.

Fourth, I would like to acknowledge Dr. Brathwaite for providing his time to evaluate my thesis and for taking the time to help me understand what I want to pursue as a career. Without him, I would not be on the path that I now know is right for me.

Fifth, I would like to acknowledge Dr. Campbell for providing time to evaluate my thesis and for pushing me to improve my writing as a scientist. My organization, while still not the best, has come much farther due to her efforts.

Finally, I would like to thank our collaborators in the Wen lab for their amazing work on the organoids and the figures provided for their survival. Their patience in waiting for my resynthesis of NPG is unmatched. I look forward to continuing to work with them.

Table of Contents

Abstract iv

1 Introduction 1

2 Methods 3

2.1 Initial Synthesis 3

2.1.1 Boc-G-OH to Boc-G-Weinreb 4

2.1.2 Boc-G-OH to HCl-NH2-G-Weinreb 4

2.1.3 HCl-NH2-G-Weinreb to Boc-PG-Weinreb 5

2.1.4 Boc-PG-Weinreb to HCl-NH2-PG-Weinreb 6

2.1.5 HCl-NH2-PG-Weinreb to Fmoc-NPG-Weinreb 6

2.1.6 Fmoc-NPG-Weinreb to Fmoc-NPG-CHO 7

2.1.7 Fmoc-NPG-CHO to NH2-NPG-CHO 8

2.2 Characterization 8

2.2.1 Transmission Electron Microscopy 8

2.2.2 X-Ray Diffraction 9

2.2.3 Organoids 9

2.3 Updated Synthesis 9

2.3.1 Synthesis of Boc trt Asn Control and General Procedure for EDC Coupling 9

2.3.2 Reduction of NPG on resin with LAH (2.0 Equivalents Approach) 10

2.3.3 Control Study of the Reduction of Boc-trt-Asn-Weinreb 11

2.3.4 DIBAL Reduction of NPG 12

3 Results 12

3.1 Synthesis 12

3.2 Transmission Electron Microscopy (TEM) 13
3.3 X-Ray Diffraction (XRD) 14
3.4 Organoids 15
3.5 Synthesis Optimization 16
4 Discussion 16
4.1 Transmission Electron Microscopy 17
4.2 X-Ray Diffraction 19
4.3 Organoids 19
4.4 Drawbacks of the Initial Synthesis 20
4.5 Assembly 21
4.6 Synthesis Optimization 25
5 Conclusions 28
6 References 30

List of Figures and Tables

Figure

0	Diagram of pyrimidinone from NFF and NPG projects	2
1	Transmission electron micrograph of NPG Assembly in Sodium Acetate	13
2	Transmission electron micrograph of NPG Assembly in Sodium Acetate	13
3	Powder X-ray Diffraction of Lyophilized NPG	14
4	Immunostains of Organoids for Apoptosis	15
6	Immunostains of Organoids for Apoptosis	15
7	Diagram of Assembly Theory 1: Ring Stacking	22
8	Diagram of Assembly Theory 2: Beta Sheet	23
9	γ-Analogues Structures	23
10	Diagram of Assembly Theory 3: Polyproline Helices	24
11	Maestro Build of NPG Assembly in Collagen Conformation	24

Table

1	Distribution of NPG Fiber Diameters	13

1 Introduction

Collagen is the most abundant protein found in the human body consisting of 30% of all human proteins. [1] Over 28 forms of triple helical forming collagen have been identified in the body playing numerous roles in maintaining chemical and physical homeostasis. [1 2] This class of proteins primary role in the extracellular matrix is, along with a complex milieu of various biomolecules, to both structurally and chemically support the cells adhered to them. Collagen is a set of large, 1.6 μm in length and 300nm in width, fibers made of covalently linked triple helices. [1 2 3] These fibers are largely insoluble in water and are thus synthesized with two globular ends, procollagen, which are cleaved extracellularly to tropocollagen, the individual triple helical unit. [2] The sequence necessary to produce this triple helical motif tends to be repeats of the trimer hydroxyproline-proline-glycine (Hyp-Pro-Gly). [4] These amino acids can form the set of tight turns necessary to hold a polyproline helix. [1 2 3 4] The triple helical unit is a strongly associated set of three polyproline II helices forming a larger supra triple helix. [5 6] This domain of these proteins confer strength to polypeptide while non-triple helical regions confer some degree of flexibility. These properties, along with helices ability to assemble into larger order structures, confers our bodies' ability to stretch and return to equilibrium rapidly. In addition to its material properties, collagen appears to have significant upkeep roles in the maintenance of neurological tissues. Collagen type VI has shown an especially important role in the prevention of apoptosis in neuronal cells. [7] UV exposed primary hippocampal cells were found to upregulate collagen VI and were saved when extracellular collagen VI was added to a knockdown strain of neural cells. [7] This points to a critical role of collagen as both a structural and chemical support for maintaining cell health.

These qualities have driven the design of numerous synthetic collagen mimetics. Most of these artificial systems utilize some form of the Hyp-Pro-Gly motif in combination with various electrically charged residues to produce an assortment of strongly associated triple helices, crystalline proteins. [5] [6] Few of these mimics attempt to recreate the more flexible dynamics of collagen though. To this end, we attempted to take advantage of previous work of Chen et al., who was able to recreate a cross beta assembly using a C-terminal aldehyde peptide asparagine-phenylalanine-phenylalanine (NFF), to produce a dynamic triple helix forming sequence. [8] Chen's work laid the foundation of selectively driving chemical equilibrium forward using the formation of secondary structures. With this system in mind, the six membered ring structure, formed by the condensation of the aldehyde and N-terminal asparagine, was first approximated as a hydroxyproline structure. From there, the sequence NPG with a C-terminal aldehyde was selected to reproduce the trimeric repeat of collagen.

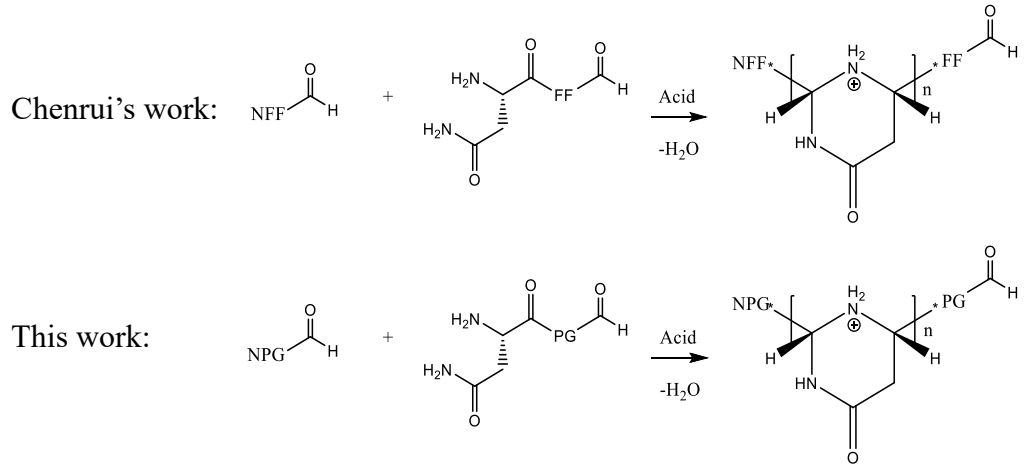

While the region chosen for this polymerization reaction is traditionally crystalline in natural collagen, the positive charge of the secondary amine in the six membered ring was designed to increase the polymers' flexibility while still maintaining the original triple helical properties. Additionally, the reversible nature of the N, N-acetal formation could allow for further dynamics.

One use for this peptide of particular interest is in brain organoid systems. Organoids are stem cell-based models for human organs grown on small scales. [9] These organs can mimic the interconnected nature of cells within an organ and can be used to model systems which lack phenotypically equivalent animal models as seen in the case of Alzheimer's disease. [9 10] Nutrient uptake is an issue in the systems however, as they lack a centralized circulatory system. Treating these organoids NPG was hoped to provide a more dynamic support structure to these brain organoids making them a more viable option for modeling. In this work, I present an initial chapter on the synthesis and characterization of the NPG C-terminal aldehyde monomer and assembly in addition to a portion on effects and future experiments on the mechanism of NPG on brain organoids. Chapter two is dedicated to the optimization of NPG synthesis and a study on the conformation adopted by the pyrimidinone ring system formed by NPG condensation.

2 Methods

2.1 Initial Synthesis

All nuclear magnetic resonance, electron spray mass spectrometry, and matrix assisted laser desorption ionization data is included in the figures section. NMR was taken on an INOVA 400, ESI was taken on Thermo Exactive Plus.

2.1.1 Tert-butoxycarbamate glycine to Tert-butoxycarbamate glycine Weinreb Amide

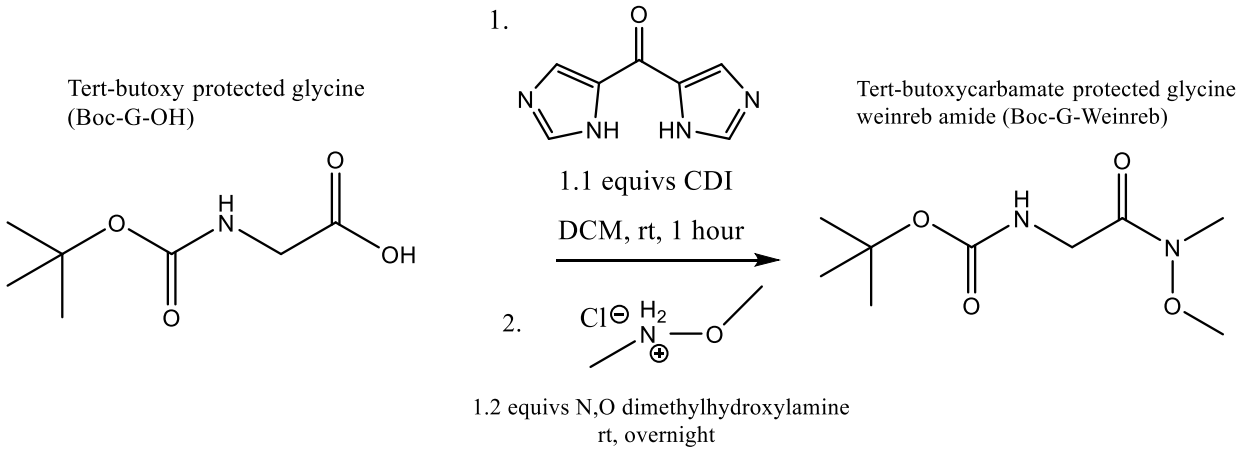

Boc-Gly-OH is added to a flask with a stir bar and dichloromethane (DCM) and is allowed to stir to a suspension. The flask is then flushed with nitrogen gas for 20 minutes. The resulting suspension is then treated with carboxydiimidazole (CDI) and is allowed to stir for 1 hour. The solution is then treated with N,O dimethylhydroxylamine and is allowed to stir overnight. The resulting solution is dried to a white powder on a rotary evaporator followed by extraction in ethyl acetate against brine. A white crystalline powder was yielded at 94.71% conversion.

2.1.2 Tert-butoxycarbamate protected glycine to glycine Weinreb amide hydrochloride salt

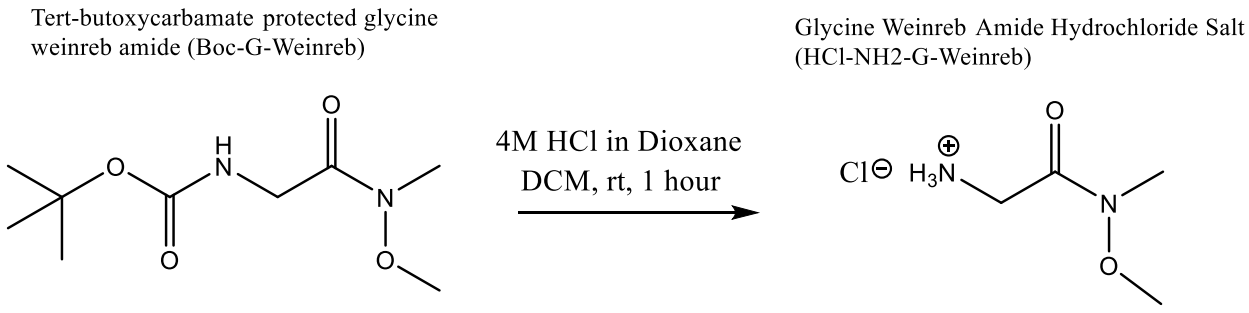

Tert-butoxycarbamate protected glycine (Boc-Gly-Weinreb) is dissolved in DCM with 4M HCl in dioxane and stirred for 1 hour at room temperature. The resulting solution is evaporated using a rotary evaporator in a yellow oil. The oil was used without further purification.

2.1.3 Glycine Weinreb amide hydrochloride salt to tert-butoxy protected proline glycine Weinreb amide

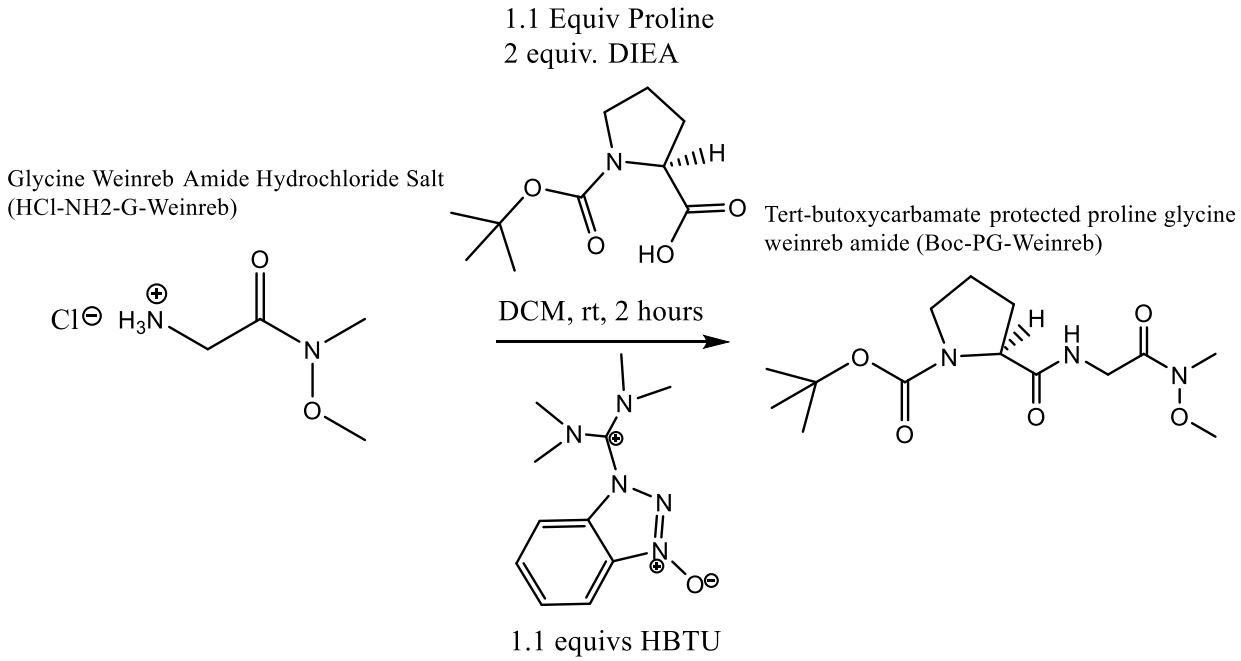

The Boc-Pro-OH was treated with hexafluorophosphate benzotriazole tetramethyl uronium (HBTU) in DCM for 1 hour. The hydrochloride salt Gly-Weinreb was dissolved in DCM followed by diisoproylethylamine (DIEA). The DCM DIEA solution was then added to the Boc-Pro-OH solution and allowed to stir for 2 hours at room temperature. The resulting solution was rotary evaporated to dryness yielding a yellow oil which was then columned using a 2:2:1 ethyl acetate: hexane: methanol on silica and was detected using ninhydrin. The resulting solid was a white powder with a yield of 88.70%.

2.1.4 Tert-butoxy protected proline glycine Weinreb amide to proline glycine Weinreb amide hydrochloride salt

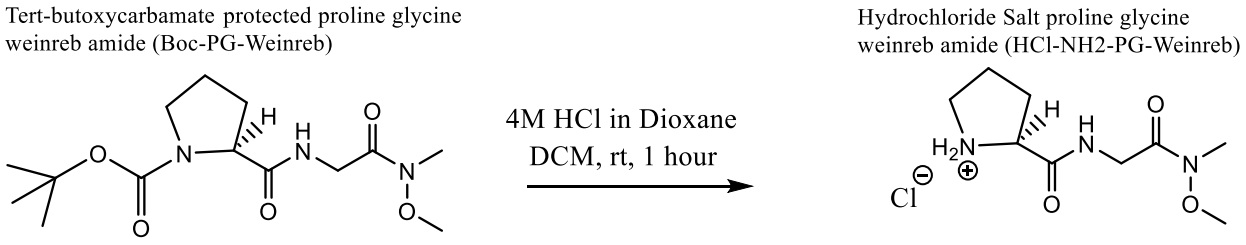

The same deprotection procedure as for Boc-Gly-Weinreb was performed for Boc-PG-Weinreb yielding a yellow oil. This was used without any further purification.

2.1.5 Proline glycine Weinreb amide hydrochloride salt to fluorenylmethoxycarbonyl protected asparagine proline glycine Weinreb amide

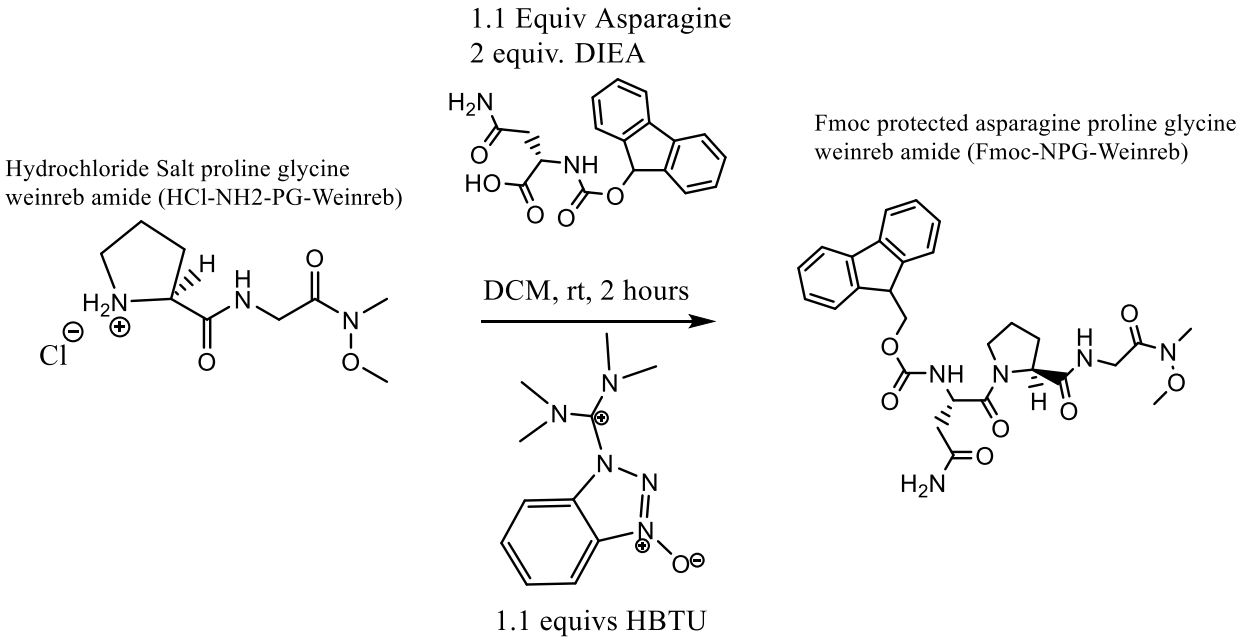

The same coupling procedure used for proline was used for Fmoc Asn OH with coupling to the hydrochloride salt of PG Weinreb. Purification was also done on a silica gel column using 2:2:1

ethyl acetate:hexane:methanol detected using UV absorption (254 nm) yielding a white solid at 29% conversion.

2.1.6 Fluorenylmethoxycarbonyl protected asparagine proline glycine Weinreb amide to fluorenylmethoxycarbonyl protected asparagine proline glycine aldehyde

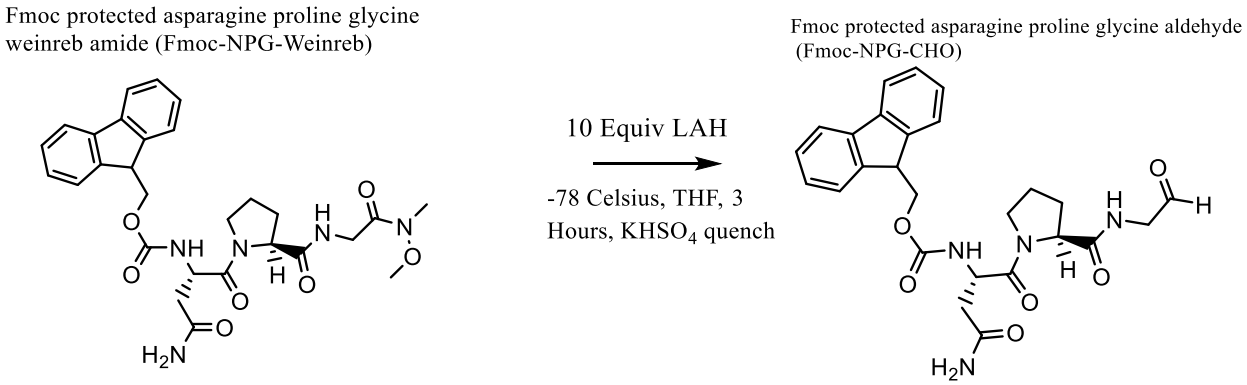

The reduction of the Weinreb amide was performed in tetrahydrofuran at -78°C. A round-bottom flask containing THF and the Fmoc NPG Weinreb was flushed with nitrogen for 20 minutes and was then placed in a dry ice and acetone bath for 20 minutes to thermally equilibrate. The resulting cooled solution was treated with 11 equivalents of 1.0 M LAH in THF and was stirred for 3 hours while kept at -78°C. [12] [13] [14] The solution was then quenched using 1.0 M $KHSO_4$ dropwise and was allowed to warm to room temperature and stirred for 30 minutes. The solution was then rotary vaporized to remove any THF followed by extraction using ethyl acetate against brine. The resulting white powder was columned using 2:2:1 (EtOAc:Hex:MeOH) and was detected using UV absorption (254 nm). The overall yield of the reaction was 60.03%.

2.1.7 Fluorenylmethoxycarbonyl protected asparagine proline glycine aldehyde to asparagine proline glycine aldehyde

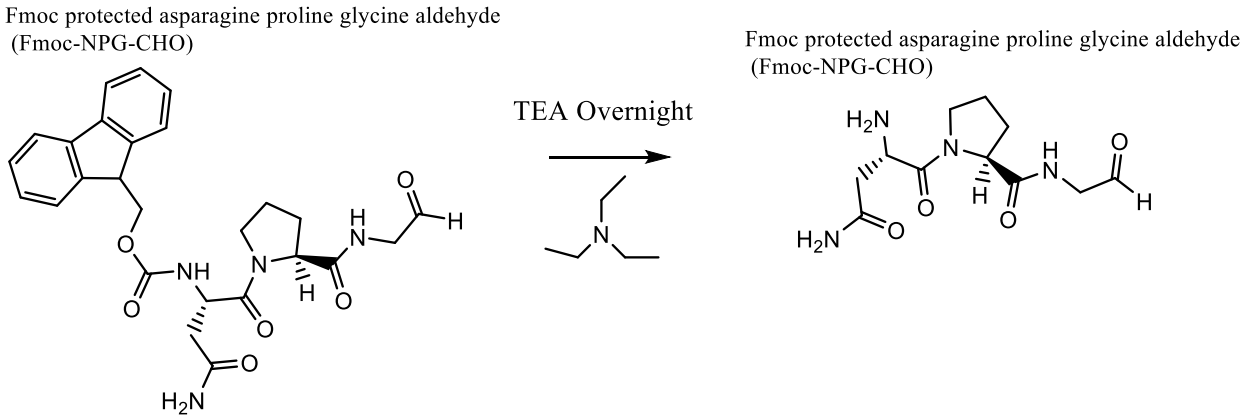

The resulting white powder was stirred in triethylamine (TEA) overnight followed by extraction into aqueous sodium acetate buffer against ethyl acetate. The solution was then evaporated on a rotary evaporator. The resulting powder was run through a C18 Sepack and was used from there. Yield not measured.

2.2 Characterization

2.2.1 Transmission Electron Microscopy

TEM was done using 200 mesh copper carbon grids with uranyl acetate dye. A 5% aqueous solution of uranyl acetate was prepared and centrifuged at 10,000x g to remove any crystalline material to the bottom of the solution. Samples were prepared by taking 10 microliters of the NPG assembly and placing it on the grid to sit for 2 minutes. The solution was then wicked off the grid using a Kimwipe through the bottom of the grid. The grid was then allowed to dry for 1 minute. The uranyl acetate was then added to the grid and allowed to sit for exactly 50 seconds

before the dye was wicked off to prevent over exposure. The images were then taken with a Hitachi H-7500 transmission electron microscope at a voltage of 75 kV.

2.2.2 X-Ray Diffraction

1.0mL of sample solution was frozen in liquid nitrogen followed by lyophilization. The remaining powder was then sent to the Emory XRD department for characterization using powder x-ray diffraction on a Bruker Apex II.

2.2.3 Organoids

Organoid samples were prepared by making 5mM solutions of NPG in 20mM phosphate buffer (pH 7.4). These samples were transferred to the Wen lab for growth in organoids with and without the NPG sample.

2.3 Updated Synthesis

2.3.1 Synthesis of tertbutoxy carbamate and triphenylmethyl protected asparagine (Boc trt Asn OH) control and General Procedure for 1-Ethyl-3-(3-dimethylaminopropyl) carbodiimide (EDC) coupling

Boc-trt-Asn-OH was suspended in DCM in a three-neck flask that was dried overnight in an oven. The resulting suspension was treated with EDC and Oxyma and was allowed to stir for 1 hour, the suspension dissolved into solution by the end of this period. N,O dimethylhydroxylamine and triethylamine, TEA was treated with 4 angstrom molecular sieves and filtered through 0.2 micron filters, was then added to the solution and was allowed to stir for

3 hours. The resulting solution was dried on rotary evaporator to a white powder followed by extraction in ethyl acetate against brine, saturated aqueous Na_2CO_3, and saturated aqueous $CuSO_4$. The resulting compound was a white crystalline solid which was measured on ^1H nuclear magnetic resonance (NMR).

2.3.2 Reduction of NPG on resin with LAH (2.0 Equivalents Approach)

Solid phase synthesis was done on Weinreb resin (substituted at 0.62 mmol/gram). Boc-trt-NPG-resin was synthesized on a 0.25 mmol scale, total of 4 syntheses, on a liberty blue synthesizer using a DIC/Oxyma based coupling scheme. The resulting resin was washed out of the reaction vessel using DCM into 4 vials. Two of these vials were poured onto filter paper in a Buchner funnel to remove the DCM and dry the resin. The Weinreb resin was then placed in a dry glass vial and was covered with two Kimwipes and was allowed to dry overnight in a desiccator. Cleavage of the resin was done by oven drying a 100mL three necked flask followed by adding a dried stir bar and the resin. The flask was then capped at all three necks and was flushed with nitrogen for 20 minutes. During this time, 20.0mL of THF was dried in two glass vials using 3 angstrom molecular sieves which were heated in an oven overnight. The solution was then added to the flask through a 0.2-micron filter to remove particulates from the sieve. The solution was then cooled to -78°C using a dry ice and acetone bath for 30 minutes. The solution was then stirred vigorously and 2 equivalents (38mg) of solid LAH was added to the center neck portion wise. The suspension was the stirred for 30 minutes to allow for dissolution of the LAH. The solution was then moved to an ice water bath and was allowed to warm to 0°C and allowed to stir for 4 hours. The resulting solution was then quenched using saturated aqueous Rochelle salt solution using an addition funnel with a gas inlet dropwise. The solution was then allowed to

warm to room temperature for 30 minutes and was then extracted in ethyl acetate and THF against saturated aqueous Rochelle salt solution.

2.3.3 Control Study of the Reduction of Boc-trt-Asn-Weinreb

The control study on the reduction conditions was carried out using the Boc-trt-Asn-Weinreb. The first study was carried out by setting up two conditions, both had 50 mg of reagent dissolved into THF in an oven-dried three-neck flask. The resulting solutions were then sparged for 20 minutes using nitrogen gas. The solutions were then cooled to -78°C and 0°C using a dry ice and acetone bath and a water ice bath, respectively. Both solutions were allowed to cool in their respective baths for 30 minutes. To each solution, 10 equivalents of solid LAH was added portion wise (40mg). The solutions were monitored by thin layer chromatography (TLC) using 1:1 (EtOAc:Hex) and were detected using KMnO4 dye. TLC was taken by pipetting 30 microliters of reaction into an Eppendorf tube followed by 500 microliters of Rochelle salt solution. 1.0 ML of ethyl acetate was then added, and the sample used for TLC was collected from the upper organic layer. The reaction was finished at 5 hours based on the appearance of two dots on the 0°C condition. The two solutions were then quenched using dropwise saturated aqueous Rochelle solution followed by extraction using ethyl acetate against saturated aqueous Rochelle salt solution. NMR was taken in $CDCl_3$ to assess for the presence of the aldehyde peak and the presence of any additional cleaving of the protecting groups. Yield: 92.6%.

2.3.4 Diisobutyl aluminum hydride (DIBAL) Reduction of NPG

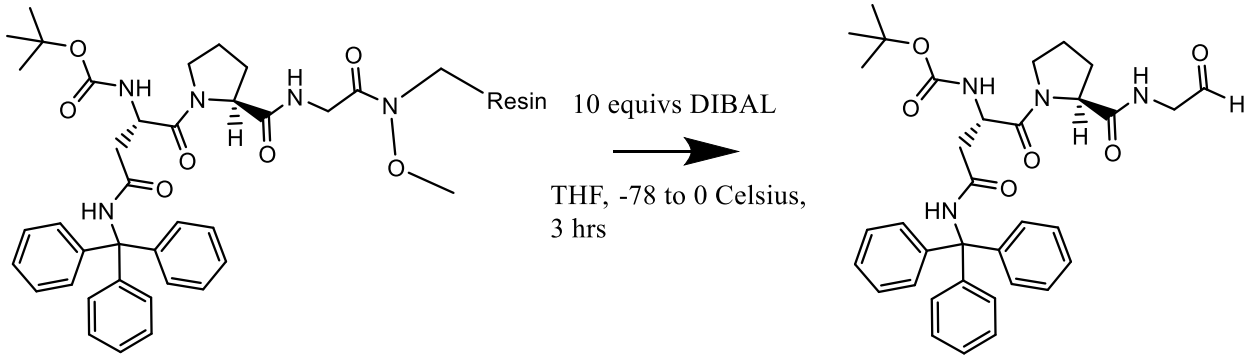

The same procedure for the LAH addition was done for DIBAL expect 1.0 mL of DIBAL was used per 1.0 Mmol of peptide synthesized on resin (10 equivalents of DIBAL).

Later adjustments were made to change the reductant from LAH to DIBAL and the equivalence number was raised from 2 to 10 with a total reaction time of three hours. The resin was then re-cleaved using the same procedure with the adjustment from 0°C to room temperature and a reaction time of 2 hours.

3 Results

3.1 Synthesis

The results of MALDI support the successful synthesis of NPG aldehyde and is further corroborated by the LC/MS data of the decamer of this polymeric structure. The 574 peak of the MALDI is the [Fmoc-NPG-CHO + Na] peak. Later ESI and H^1 NMR results corroborated the results of the synthesis up to the tripeptide Weinreb amide, but the final ESI did appear to agree with this result.

3.2 Transmission Electron Microscopy (TEM)

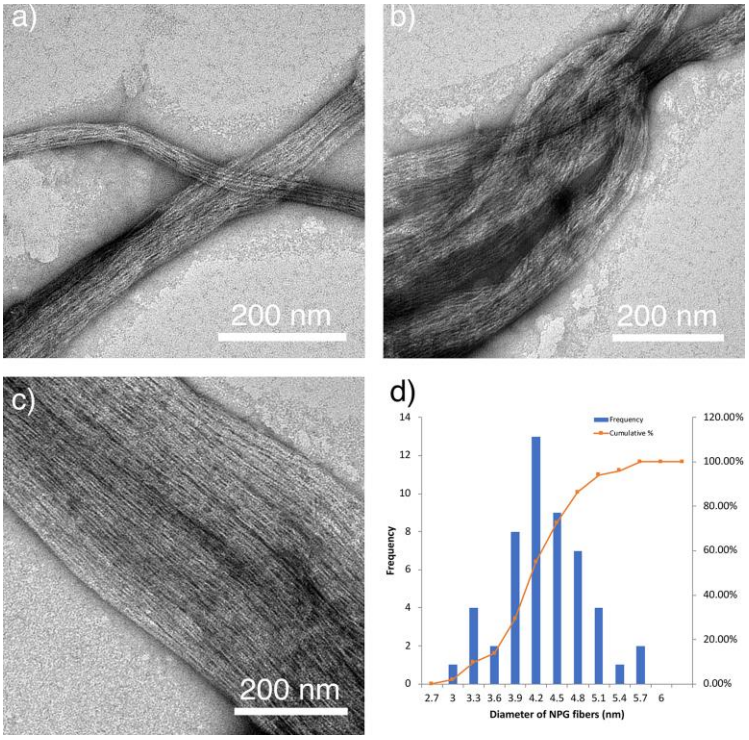

Figure 1: TEM of NPG Assembly from Aqueous Solution. The samples shown above were collected 14 days post the initial dissolution of NPG. Bundled fibers are shown in a), b), and c). In b) the bundles have begun to twist into a larger structure.

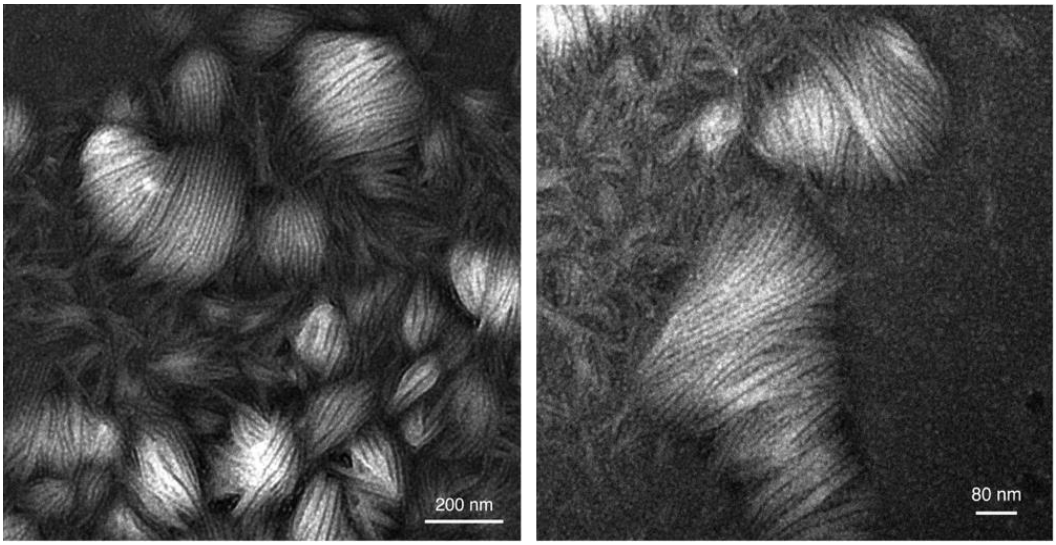

Figure 2: TEM of NPG Assembly from Acetonitrile Solution. The samples shown above were collected 14 days post the initial dissolution of NPG. Bundled in both a) and b). The new structures formed are referred to as 'balls of yarn.'

The electron micrographs of NPG aldehyde show a fibrous structure that is able to twist into larger order configurations. The median diameter of the individual fibers is 4.2 nm and has a standard deviation of 0.6 nm (Fig. 1). The individual fibers appear to assemble together into a 'bundle structure' and with sufficient conditions, i.e., a 50% acetonitrile water solution, these bundles begin to twist into one another to form a 'ball of yarn.' The decamer was the predominant oligomer based on LC/MS as the 852-peaks showed spacings of 0.33 between peaks indicating a charge of +3 on the system which means the molecular weight of the ion is instead 2556 (Fig. S13).

3.3 X-Ray Diffraction (XRD)

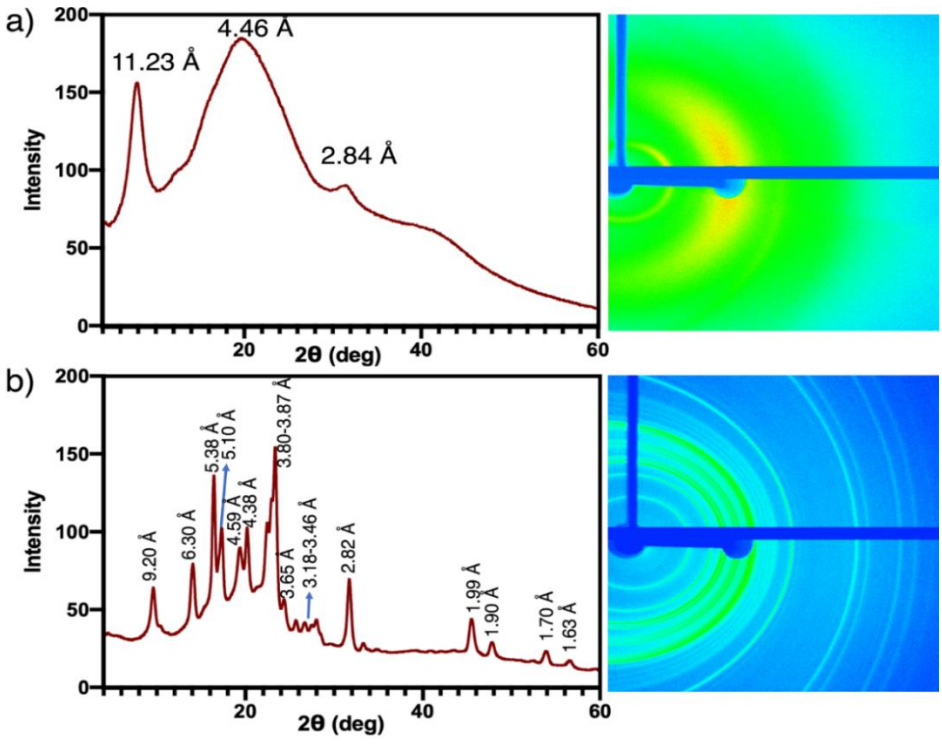

Figure 3: Xray diffraction of Lyophilized NPG 14 days Past Dissolution. Samples of NPG were frozen in liquid nitrogen then put under vacuum to remove all solvent. The powder was sent to the Emory XRD department along with a sample of bovine collagen. NPG appears crystalline. Bovine collagen appears nonhomogeneous.

The bovine tendon collagen appeared to have a wide distribution of distances between atoms with peaks at 11.23 angstroms, 4.46 angstroms, and 2.84 angstroms (Fig. 2). The NPG assembly takes on numerous more sharp and precise distances which points to a more crystalline material (Fig. 2). The 4.38 and 9.20 peaks appear to be the closest to those found in natural collagen (Fig. 2).

3.4 Organoids

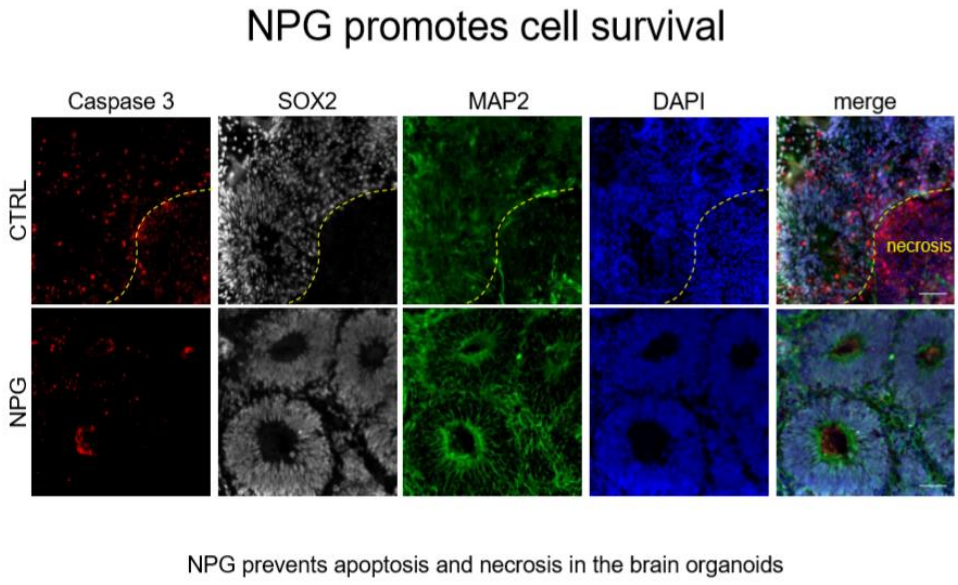

Figure 4: Brain organoids one month of growth with and without NPG. The NPG raised samples appeared to survive more in the center cells as shown by the reduction in activity of all immunostains. except for caspase3 which showed increased apoptosis. Data and figure collected by Dr. Zhexing Wen and Xianzhen Zheng.

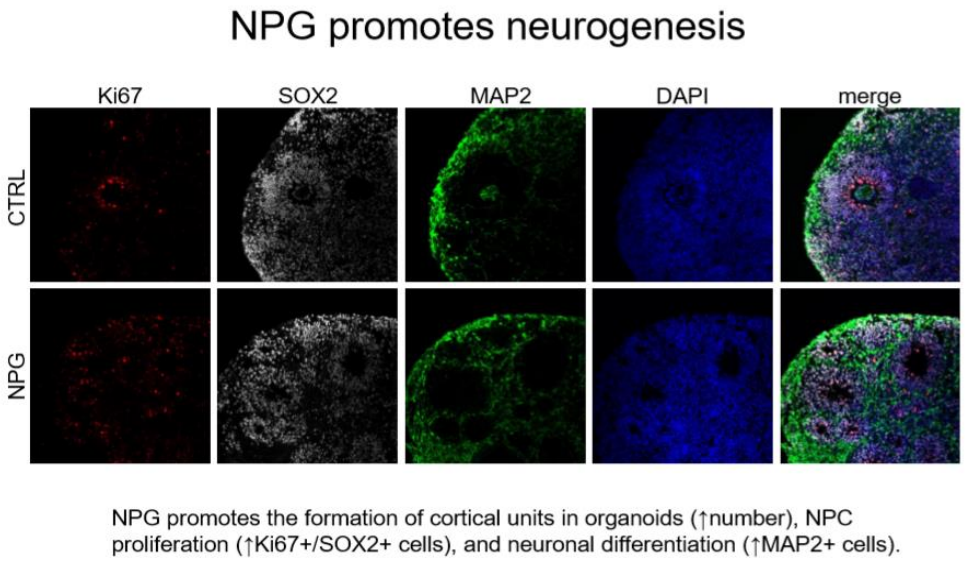

Figure 5: Brain organoids one month of growth with and without NPG. The NPG raised samples appeared to survive more in the center cells as shown by the reduction in activity of all immunostains. except for ki67 which showed increased levels of differentiation by the cells. Data and figure collected by Dr. Zhexing Wen and Xianzhen Zheng.

The organoids results show a decrease in caspase 3 activity in the inner cells of the organoid while SOX2, Nestin, Ki67, MAP2, and DAPI all increased in the inner brain organoids in the immunostaining assay (Figs. 4 and 5).

3.5 Synthesis Optimization

The final synthesis of the aldehyde of Boc-trt-NPG gave a relatively low yield but was able to produce the aldehyde with minimal side cleaving of the amides. Purification and isolation of the desired aldehyde compound is still ongoing but will allow for higher yield routes to be explored and more general peptide cleavage procedures to be found.

4 Discussion

4.1 Transmission Electron Microscopy

When placed into solution, NPG appears to undergo polymerization to a decamer state which then assembles to higher order structures. It is uncertain if there are longer polymers that form but no polymers shorter than 10 NPG units long were noted based on LC/MS results. The calculated 2556 peak indicates a decamer of NPG with a geminal diol terminus. All these structures form on a basic fiber which undergoes further association to yield bundled fibers (Figs. 1 and 2). Based on TEM grids taken from NPG samples prepared in sodium acetate buffer, DI water, and water/acetonitrile NPG appears to be able to undergo polymerization in a variety of solvent environments (Figs. 1 and 2). It is especially interesting as previous work by Chen had shown almost no formation of the aminal ring when in aqueous solution. [8] This novel behavior from NPG may be the result of either phase separation in solution driving chemical equilibrium, or through sequestration of the monomers into the polymeric form. In the first hypothesis, a hydrophobic core of the monomer forms a separate phase from the bulk aqueous solvent. The lack of water in this environment drives the monomers to polymerize and later assemble into fibers through association of the individual strands. The second hypothesis posits that the secondary structures formed by the polymer may create an environment which prevents the reverse hydrolysis of the polymer. The structure would then continue to lengthen and form higher order bundled structures. Based on the phase separated globules formed by Chen's NFF system, the first hypothesis is less likely. [8] The NFF system underwent polymerization to only a trimer and had access to far greater hydrophobicity while the NPG system is able to attain a decamer. It may also be a combination of these two factors based on the structures observed. Some phase separated spheres were observed in the immature NPG samples which does indicate some degree of phase separation (Data not provided). The initial phase separation may be

necessary to form short oligomers which then associate to drive further polymerization. This may be tested through more rigorous testing of the molecular weights available in solution across time coupled together with Raman spectroscopy. Raman spectroscopy can be used to detect changes in the local environment of the amide bond while maintaining the sample in an aqueous environment, though detection of the methylene group of the asparagine side chain should be more intense owing to the change in polarizability of the orbital and its direct action in the pyrimidinone. [21] Matching the length of structures available with the degree of structure achieved may provide further insight into the nature of the polymerization reaction.

It is also worth noting the further degree of assembly primarily noted in acetonitrile water mixture sample. Within the aqueous sample, bundled fibers were the primary higher order structure noted, while the “ball of yarn” or suprabundled fiber sample was noted in the acetonitrile solution. This may result from the interaction of the solvent with the assembly or through further polymerization as mass spectrometry was not run on this sample. The solvent interaction approach would indicate a decrease in the number of available polar interactions may encourage the assembly to self-associate to a higher degree. In the polymerization approach, less available water may encourage the forward polymerization reaction and allow for longer twists in the overall structure. Electrospray ionization mass spectrometry (ESI) on the mature acetonitrile assembly can help to eliminate or support the second hypothesis while a calorimetric study of the structure’s energy in acetonitrile vs. aqueous solvent may either support or refute the first hypothesis.

4.2 X-Ray Diffraction

The largest difference between the two spectra was the more dispersed spacing of the collagen while the NPG aldehyde was more crystalline (Fig. 3). Both have large amounts of larger distances though this is not unusual in any higher order structure. The lack of 11.23 angstrom distance indicates the distances between strands is not as large as seen in collagen. The very similar 2.82 angstrom and 2.84 angstrom distance seems noteworthy but likely corresponds to the spacing of sodium chloride likely in the sample (Fig. 3). If the sample is triple helical in nature, it is almost certainly not in the same registry or conformation as seen in natural collagen. A similar set of distances has been observed in other collagen types. [11]

4.3 Organoids

Assays for NPG in brain organoid systems were run by the Wen lab. A sample of 1.0 mM NPG was provided in 7.4 pH 20 mM PBS buffer and was added to the growing organoid cultures. The results of which were stained using immunostaining of Sox2, Nestin, MAP2, Ki67, and Caspase-3 along with a DAPI dye. SOX-2 is an important transcription factor in the upkeep of pluripotency in stem cells. [15] Nestin is an intermediate fiber important in the radial growth of neuronal axons. [15] MAP2, microtubule associated protein, is also affiliated with the cytoskeleton. [16] It is particular to neuronal cells and is therefore immunoassayed to help identify morphology. Ki67 is used to determine the proliferation of cells as it is found in division and can be used to assess whether the organoid is actively growing. [16] Caspase-3 is affiliated with apoptotic activity signaling cell death. [17] Activity of this indicates the organoid cells are actively dying. DAPI is a DNA dye for AT rich regions, useful to stain the nuclear region of organoid cells. [16 17] The results of this fluorescence indicate an increased amount of cellular proliferation and reduced

apoptosis in the NPG treated sample as compared to a control (Figs. 4 and 5). The precise reasoning for this increased survival is currently unknown. One potential mechanism may be a decreased viscosity of the extracellular fluid which can increase the flow of nutrients into deeper cells. If this is the case, a rheological study of the isolated solution should indicate a decreased viscosity. [18] This may also explain the increased proliferation of neural progenitor cells detected using ki67 as seen in below (Fig. 5). Another mechanism may be activation of the Akt/Phosphatidylinositol 3-kinases (PI3K) pathway as has been noted by exposure to collagen VI results in upregulation of this pathway saving apoptotic phenotypes. [4] Running a western blot to detect the upregulation of this pathway would also be of interest. A more baseline study that would yield further information would be the introduction of ^{15}N labeled amino acids into the NPG sequence followed by culturing of the organoid. [19] The organoid and solution would then be centrifuged and decanted followed by an NMR. This would determine whether the amino acids remained primarily extracellular or if the monomers are capable of partitioning into the cellular fluid.

4.4 Drawbacks of the Initial Synthesis

The synthesis of NPG started with a manual coupling liquid phase approach; the coupling agent used was HBTU due to its availability. CDI was selected as the coupling agent for converting glycine to the Weinreb amide as there was no concern of epimerization from the addition of carboxylate activating groups, which tend to be electron withdrawing and thus lower the pKa of the alpha proton. Synthesis was done stepwise using boc protecting groups as HCl could readily be removed through evaporation. The main benefit of this approach was the scale this synthesis. Reactions could take place on gram scales as opposed to the usual tens of milligrams produced

through solid phase automated synthesis. The final reduction was done using 1.0 M LAH in THF with 10 equivalents, a standard regularly referred to in the literature, followed by quenching with 1.0 M $KHSO_4$. By far, the largest drawback of this reaction was the reduction in yield from carrying out column chromatography on each step of the reaction. The side product of the coupling reaction and the base used, DIEA, could not be removed using liquid-liquid extraction so columns had to be run to purify the peptides. The excess of coupling steps led to a significant reduction in the rate of synthesis and was further compounded by the difficulties affiliated with column purification of amines. Silica is mildly acidic and tends to protonate amines leading to high affinity for the solid phase and a significant need for more polar mobile phases. This was not an issue at first and NPG was synthesized according to MALDI mass spectrometry; however, the certainty of this synthesis came into question as the ESI did not yield the appropriate mass for the compound and NMR was not initially taken. In contrast, LC/MS did yield the correct masses. The assembly is most likely the result of NPG polymerization, but the doubts raised over ESI and the lack of NMR warrant reverification of the product and likely an overhauling of the synthesis to produce a more streamlined approach.

4.5 Assembly

The assembly of NPG into the observed structures may follow a variety of pathways. The intended pathway was through adoption of a triple helix motif forming three individual poly proline 2 helices which form into larger higher order complexes. Other potential motifs NPG may adopt could be cyclic ring structures or cross beta sheets. In the cyclic ring structure theory, the molecules of NPG are reacting N to C terminus to form a closed loop similar to a macrocycle (Fig. 6).

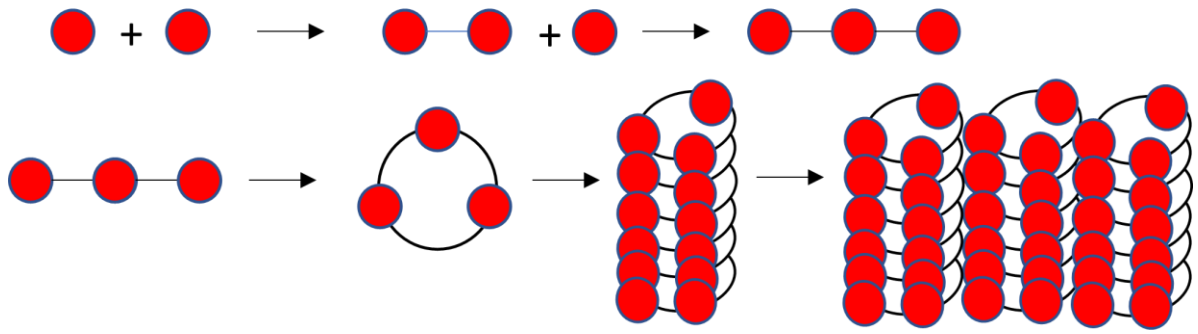

Figure 6: Theory 1 of NPG Assembly: Tubes. Within this model, the NPG monomers polymerize then cyclize to form rings which stack upon one another and then proceed to bundle to form higher order structures. The twists may result from offsets in the stacking. Red circles are NPG.

These rings could then stack to form larger fibers which may then cross with other strands to from the bundled fibers observed on the TEM grid (Figs. 1 and 2). The hole formed by the macrocycles would be too small for the assembly to function as a nanotube which would explain the lack of said observed structures under this theory.

Another approach may instead be the formation of cross beta sheet with a unique morphology (Fig. 7).

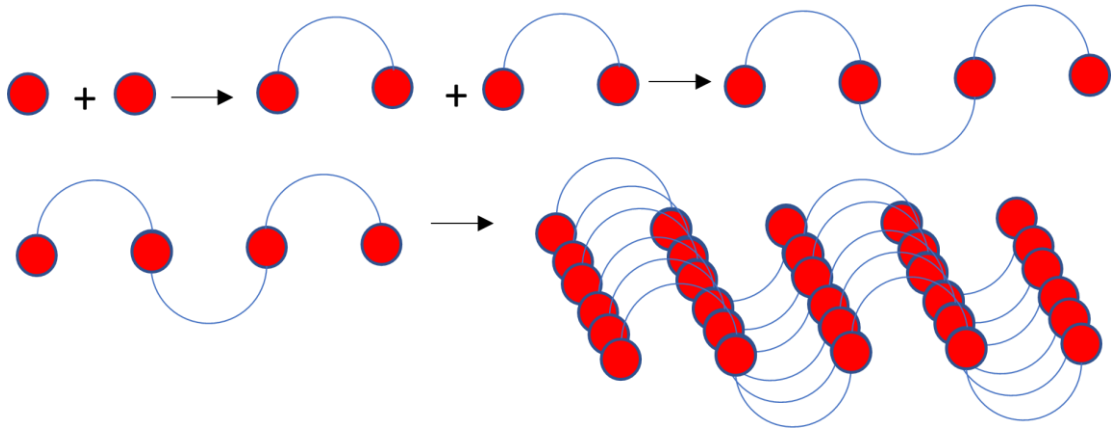

Figure 7: Theory 2 of NPG Assembly: Beta Sheet. Within this model, the NPG monomers polymerize but the six membered pyrimidinone forms a loop that causes the system to form a cross beta sheet. This is the structure that Chen characterized in her original work.

The similarity to an oxopiperazine ring analogue formed by the condensation of two monomers does bear a semblance to turns observed in beta sheets which may support this hypothesis (Fig. 8). [20] The final theory posits the formation of a triple helical structure (Figs. 9 and 10).

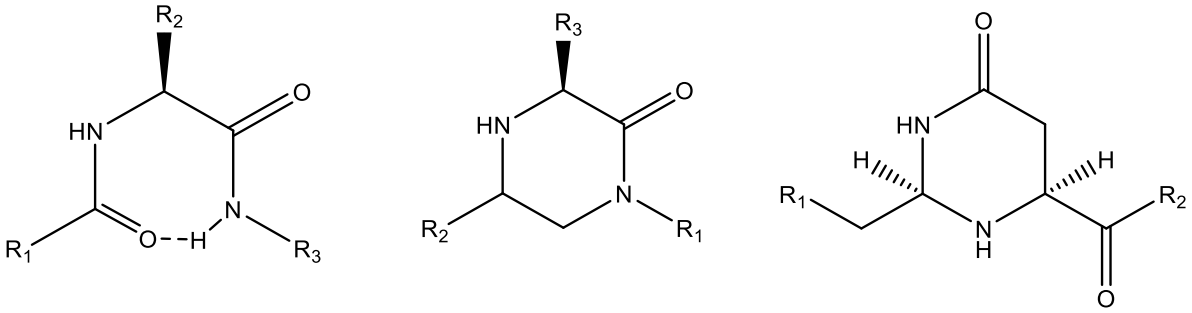

Gamma-turn Oxopiperazine Pyrimididone (This work)

Figure 8: Theory 2 of NPG Assembly: Beta Sheet. The first structure is the generic form of a gamma turn, the second is a common chemical motif used to replicate the gamma turn without using amino acids. The last structure, from this work, shows the similarity to both indicating turns may form consistently.

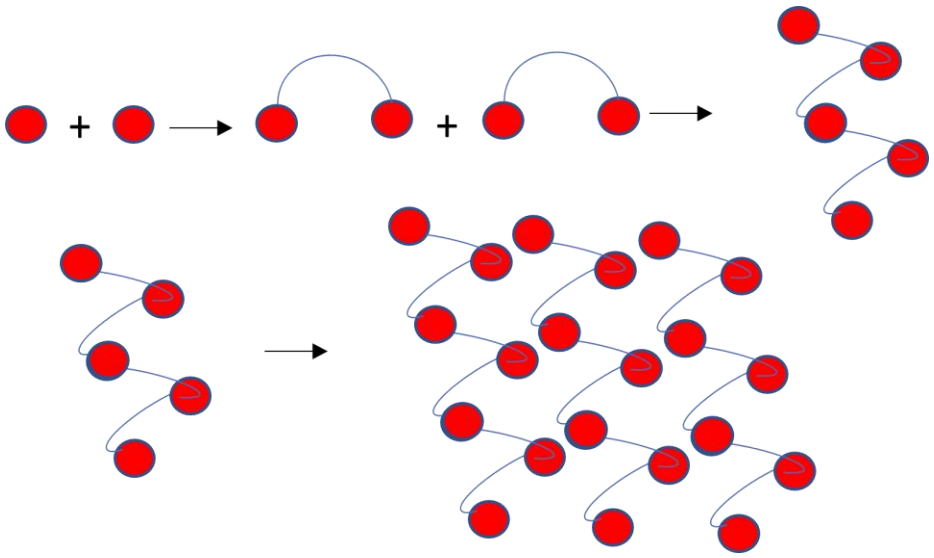

Figure 9: Theory 3 of NPG Assembly: Triple Helix. In this model, the turns from theory 2 remain, but are offset along the z-axis to form a twisting spiral structure. This strand aggregates, potentially to a triple helix, and forms the structures seen. Twisting would arise from offsets upon each turn.

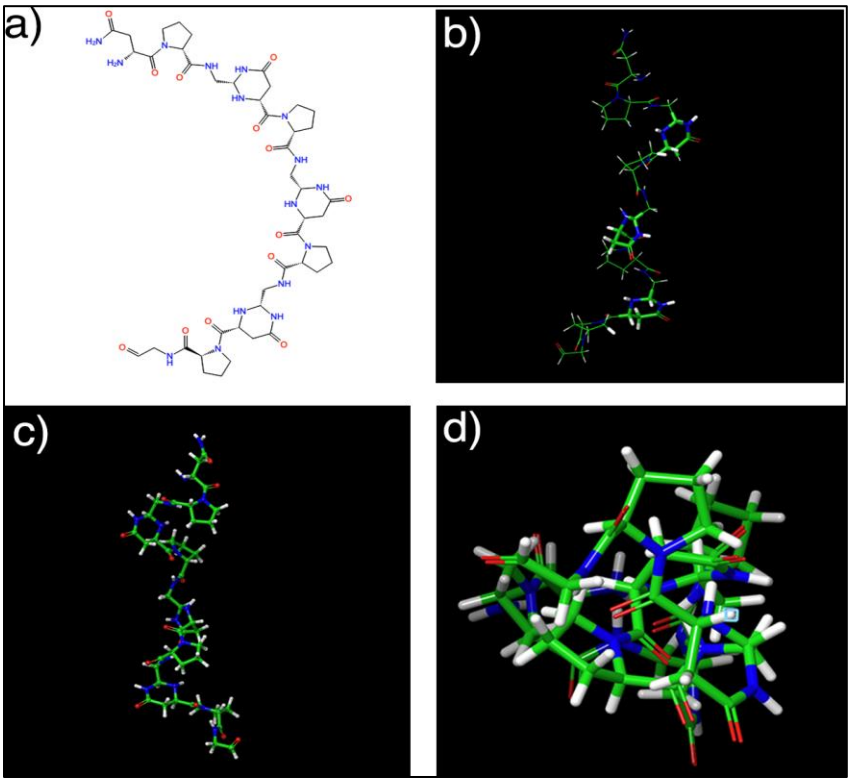

Figure 10: Theory 3 of NPG Assembly: Triple Helix. Shown above is a maestro model for the offset system. In a) is the chemical structure of the polymer form. In b) and c) are side views of the structure. In d) is the top-down view of the structure.

The peptide utilizes the gamma turns to fold upwards upon itself to form a spiral structure. These spirals then condense to form the fibers observed (Fig. 9). In order to delineate which theory is most supported, an ESI on the final assembly may be a solution. Cyclic rings produce a unique molecular weight which can be measured. If this does not hold true, the length of the strand may still be discerned by ESI. The conformation of the strands may be measured through isotopic labeling of the asparagine amide N to ^{15}N followed by solid state NMR. The distance and potential registry of the assembly can then be determined using the distances measured through said experiment. A thioflavin T or congo red assay can also be used to help delineate if the structure formed is, in fact, a cross beta sheet as enhanced fluorescence of the dye should be observed. Finally, a set of cross seeding experiments could help to delineate between the final two hypotheses. Sequences known to form cross beta sheets could be introduced into solution alongside NPG in one solution and a sequence for the triple helix in the other. If the rate of formation of the structure is accelerated in either solution, NPG may prefer to adopt that form of structure.

4.6 Synthesis Optimization

Post the initial characterization, the synthetic scheme was modified to improve the time needed and purity of the final compound. This was initially by replacing hydroxybenzyl triazole uronium (HBTU) with diisopropyl carodiimide (DIC) and oxyma pure as the urea byproduct of the reaction was more readily extracted using a separatory funnel. This however did not proceed as hoped as thin layer chromatography several hours later indicated nearly no conversion when coupling amino acids, specifically glycine Weinreb to proline. This could have been remedied through the use of increased reaction times as other amide coupling reactions can be run on the

order of 14-16 hours when done using carbodiimide reactions as compared to HBTU based coupling. The rapidity of HBTU is what lead to this initial confusion. As a result of this setback, synthesis was shifted to a solid phase automated approach using a Weinreb resin. While this tends to produce less compound overall as the quantity is limited to the surface area of the resin, the purity is far higher, and synthesis is far faster as impurities can be easily washed off and the reaction is heated using microwaves. The first attempt at solid phase synthesis was done using a control peptide NPG on Wang resin both for later testing and as a means of learning this technique. The peptide was cleaved off the resin using a trifluoroacetic acid (TFA) solution with ethylene dithiol, thianisole, and anisole to catch any radicals formed. The synthesis was successful, and the peptide was isolated on HPLC. With the general synthesis procedure completed cleavage procedure to remove NPG from the Weinreb resin was designed to copy the initial approach used to synthesize NPG, 10 equivalents of solid LAH, using a THF solvent system with a $KHSO_4$ quench. The solid phase approach initially failed as well though. Extraction was done using ethyl acetate against brine and neither layer appeared to hold a compound of the appropriate molecular weight according to mass spectrometry and no aldehyde proton shift was detected on H^1 NMR, meaning there was no NPG aldehyde in the reaction vessel at all. It became evident that a set of conditions needed to be screened to optimize the synthesis as the peptides were synthesized on the Weinreb resin. First, the Boc-trt-asn-Weinreb was used to test a variety of temperatures needed to produce the desired compound. It was found that -78°C appeared to produce only one dot by TLC while a number of dots formed in the 0°C sample though NMR of both samples indicated the formation of aldehyde (Appendix, Fig. S8). The -78°C condition was selected to attempt another reduction of the Weinreb amide resin. In addition, the quenching solution was switched from $KHSO_4$ to a saturated solution of sodium

potassium tartrate to avoid potential deprotection of the acid labile tert-butoxy carbonyl and trityl protecting groups. This had the added effect of causing THF to separate from the aqueous phase which may prevent the peptide from partitioning into the incorrect layer. The reduction was run and checked on H^1 NMR yielding no aldehyde proton shift. ESI showed an incredibly small quantity of the aldehyde had formed with a mess of spectrum containing numerous peaks. At this point, the reduction was retested on the asparagine control system changing the number of equivalents of LAH in hopes of preventing overreduction. Running the reduction at -78°C and 0°C both with 1.1 equivalents of LAH and 2 equivalents of LAH yielded aldehyde only in the 2 equivalents at 0°C condition (Appendix, Fig. S9). This was then run on the NPG charged resin, but no solid was isolated after extraction. As a last attempt, the reductant was switched from LAH to diisobutyl aluminum hydride (DIBAL) and 10 equivalents was used at 0°C in hopes of reducing side reductions while still producing the aldehyde. A white solid was isolated with a 33% yield from the resin (Appendix, Fig. S10). Purification of the powder was then attempted on HPLC, but the compound would not dissolve in any concentration of acetonitrile, likely due to its extreme hydrophobicity. Instead, the focus became to remove the protecting groups while still preventing polymerization.

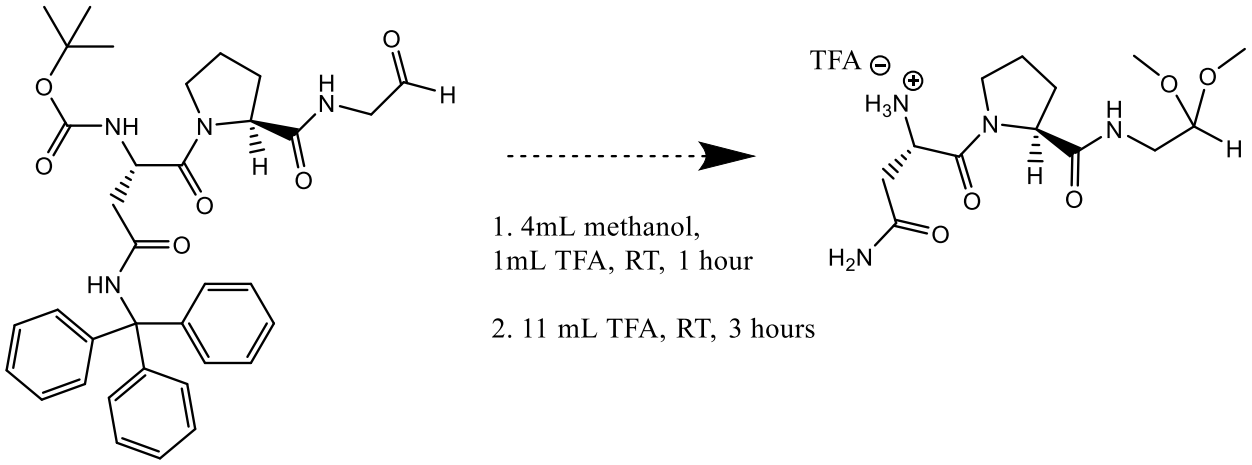

The proposed approach for this synthetic pathway is through formation of the dimethoxy acetal in methanol and TFA initially followed by an excess of TFA to remove the boc and trityl groups, like how deprotection of the NPG control was done. This should also be adaptable to a number of other peptides as most side chain protecting groups are acid labile. The only potential issue may be the exchange of the dimethyl group in acid which can be switched for ethylene glycol to increase stability if needed.

5 Conclusions

NPG forms a fascinating array of complexes that significantly deviate from structures observed by Chen. [8] The characteristics of this assembly point to a fibril as the basic unit of assembly which forms higher order bundles. These bundles, if formed in sufficient quantities undergo final transition to a 'ball of yarn' a highly interwoven network of fibers. Said fibers appear to be more crystalline based on the X-ray diffraction data. One of the most interesting finds was the results on the interaction of the system with brain organoids. The decreased apoptosis and increased survival of inner cells indicates some impact on the part of NPG. It remains to be seen when compared to a non-polymerizing equivalent whether this effect is from the assembly or merely through the diffusion of amino acids into the cells. Even further work using ^{15}N can discern the localization of NPG in brain organoids or the extracellular fluid along with fluorescence measurements to determine the impact of NPG on the viscosity of the surrounding solution. Optimizing and definitively confirming the synthesis of NPG is still an ongoing process. The current state of synthesis allows for proper production of the peptide sequence thanks to automated solid phase synthesis, and proper cleavage of the peptide using 10 equivalents of 1.0

M DIBAL in toluene at 0°C for 3 hours followed by a saturated Rochelle Salt solution quench. This method is readily adaptable to any peptide on solid phase synthesis. The new proposed cleavage for the final step is additionally applicable to any solid phase synthesis peptide. A cold ether precipitation after deprotection should further make the process applicable to a wide variety of peptide targets.

6 References

1. Ricard-Blum, S., The collagen family. *Cold Spring Harb Perspect Biol* **2011,** *3* (1), a004978.

2. Gregorio, I.; Braghetta, P.; Bonaldo, P.; Cescon, M., Collagen VI in healthy and diseased nervous system. *Disease Models & Mechanisms* **2018,** *11* (6), dmm032946.

3. Goldberga, I.; Li, R.; Duer, M. J., Collagen Structure–Function Relationships from Solid-State NMR Spectroscopy. *Accounts of Chemical Research* **2018,** *51* (7), 1621-1629.

4. Bella, J.; Eaton, M.; Brodsky, B.; Berman, H. M., Crystal and Molecular Structure of a Collagen-Like Peptide at 1.9 Å Resolution. *Science* **1994,** *266* (5182), 75-81.

5. Sarkar, B.; O'Leary, L. E. R.; Hartgerink, J. D., Self-Assembly of Fiber-Forming Collagen Mimetic Peptides Controlled by Triple-Helical Nucleation. *Journal of the American Chemical Society* **2014,** *136* (41), 14417-14424.

6. Rele, S.; Song, Y.; Apkarian, R. P.; Qu, Z.; Conticello, V. P.; Chaikof, E. L., D-Periodic Collagen-Mimetic Microfibers. *Journal of the American Chemical Society* **2007,** *129* (47), 14780-14787.

7. Cheng, I. H.; Lin, Y. C.; Hwang, E.; Huang, H. T.; Chang, W. H.; Liu, Y. L.; Chao, C. Y., Collagen VI protects against neuronal apoptosis elicited by ultraviolet irradiation via an Akt/Phosphatidylinositol 3-kinase signaling pathway. *Neuroscience* **2011,** *183*, 178-188.

8. Chen, C.; Tan, J.; Hsieh, M.-C.; Pan, T.; Goodwin, J. T.; Mehta, A. K.; Grover, M. A.; Lynn, D. G., Design of multi-phase dynamic chemical networks. *Nature Chemistry* **2017,** *9* (8), 799-804.

9. Qian, X.; Jacob, F.; Song, M. M.; Nguyen, H. N.; Song, H.; Ming, G.-l., Generation of human brain region–specific organoids using a miniaturized spinning bioreactor. *Nat Protoc* **2018,** *13* (3), 565-580.

10. Neff, E. P., Animal models of Alzheimer's disease embrace diversity. *Lab Animal* **2019,** *48* (9), 255-259.

11. Okuyama, K., Revisiting the molecular structure of collagen. *Connect Tissue Res* **2008,** *49* (5), 299-310.

12. Sibi, M. P., CHEMISTRY OF N-METHOXY-N-METHYLAMIDES. APPLICATIONS IN SYNTHESIS. A REVIEW. *Organic Preparations and Procedures International* **1993,** *25* (1), 15-40.

13. Wilson, T. A.; Tokarski, R. J.; Sullivan, P.; Demoret, R. M.; Orjala, J.; Rakotondraibe, L. H.; Fuchs, J. R., Total Synthesis of Scytonemide A Employing Weinreb AM Solid-Phase Resin. *Journal of Natural Products* **2018,** *81* (3), 534-542.

14. Giltrap, A. M.; Cergol, K. M.; Pang, A.; Britton, W. J.; Payne, R. J., Total synthesis of fellutamide B and deoxy-fellutamides B, C, and D. *Mar Drugs* **2013,** *11* (7), 2382-97.

15. Trisno, S. L.; Philo, K. E. D.; McCracken, K. W.; Catá, E. M.; Ruiz-Torres, S.; Rankin, S. A.; Han, L.; Nasr, T.; Chaturvedi, P.; Rothenberg, M. E.; Mandegar, M. A.; Wells, S. I.; Zorn, A. M.; Wells, J. M., Esophageal Organoids from Human Pluripotent Stem Cells Delineate Sox2 Functions during Esophageal Specification. *Cell Stem Cell* **2018,** *23* (4), 501-515.e7.

16. Xie, B.-Y.; Wu, A.-W., Organoid Culture of Isolated Cells from Patient-derived Tissues with Colorectal Cancer. *Chin Med J (Engl)* **2016,** *129* (20), 2469-2475.

17. Bode, K. J.; Mueller, S.; Schweinlin, M.; Metzger, M.; Brunner, T., A fast and simple fluorometric method to detect cell death in 3D intestinal organoids. *BioTechniques* **2019,** *67* (1), 23-28.

18. Ramirez, B.; Durst, M. A.; Lavie, A.; Caffrey, M., NMR-based metabolite studies with 15N amino acids. *Scientific Reports* **2019,** *9* (1), 12798.

19. Herrero, S.; García-López, M. T.; Latorre, M.; Cenarruzabeitia, E.; Del Río, J.; Herranz, R., 2-Oxopiperazine-Based γ-Turn Conformationally Constrained Peptides: Synthesis of CCK-4 Analogues. *The Journal of Organic Chemistry* **2002,** *67* (11), 3866-3873.

20. Vyšniauskas, A.; Qurashi, M.; Gallop, N.; Balaz, M.; Anderson, H. L.; Kuimova, M. K., Unravelling the effect of temperature on viscosity-sensitive fluorescent molecular rotors. *Chem Sci* **2015,** *6* (10), 5773-5778.

21. Martinez, M. G.; Bullock, A. J.; MacNeil, S.; Rehman, I. U., Characterization of structural changes in collagen with Raman spectroscopy. *Applied Spectroscopy Reviews* **2019,** *54* (6), 509-542.

Supplementary Table of Contents

Figure S1. Boc-G-Weinreb 35

Figure S2: HCl-NH_2-G-Weinreb 37

Figure S3: Boc-PG-Weinreb NMR and ESI 38

Figure S5: HCl-NH_2-PG-Weinreb 40

Figure S6: Fmoc-NPG-Weinreb 41

Figure S7: Fmoc-NPG-CHO 43

Figure S8: Control NPG 45

Figure S9:10 Equivalents LAH on Control Temperatures 46

Figure S10: 10 Equivalents LAH on Boc trt NPG Resin 48

Figure S11:1.1 and 2.0 Equivalents LAH on Control 49

Figure S12: 10 Equivalents DIBAL on Boc-trt-NPG Resin 51

Figure S13: HPLC and Mass Spec Data for NPG Assembly 52

Figure S1. Boc-G-Weinreb

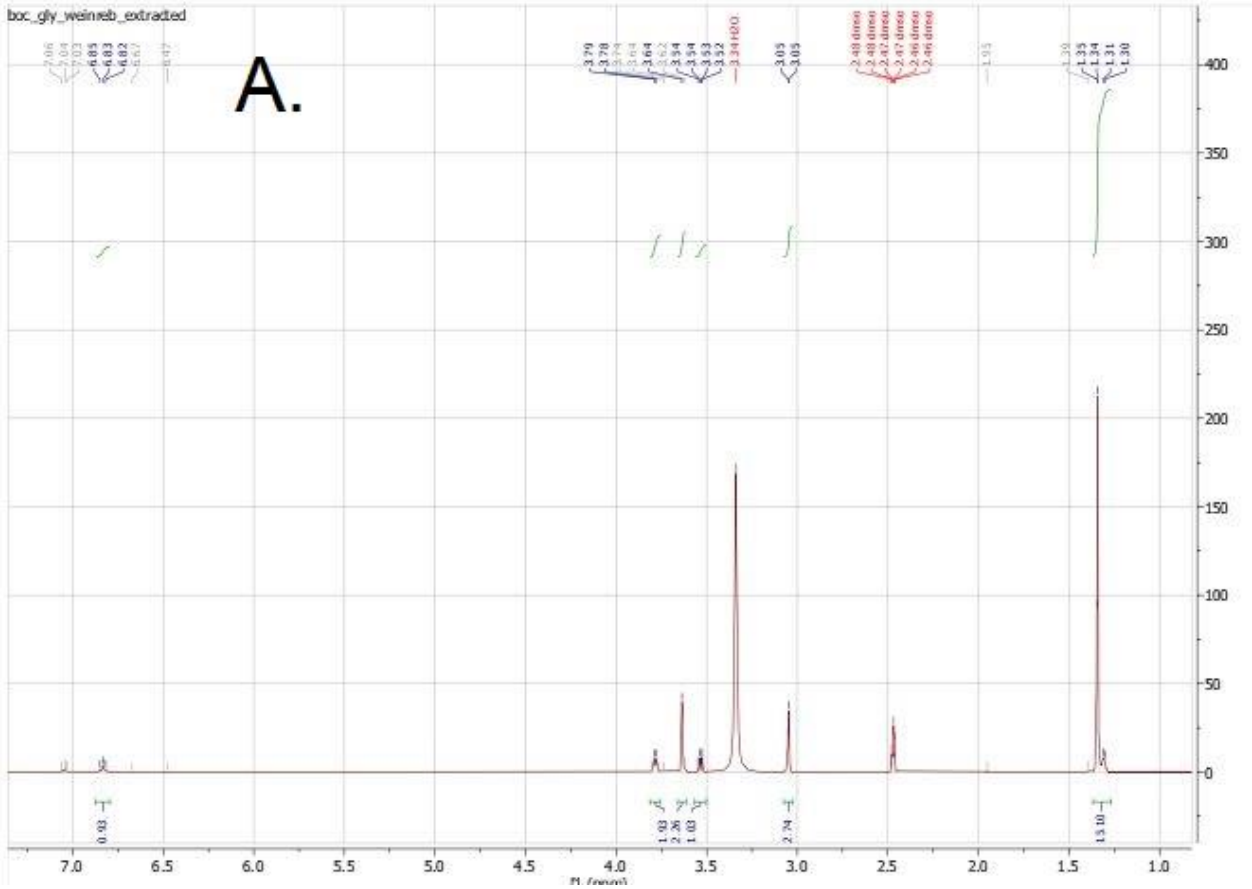

H^1 NMR spectra of Boc-Gly-Weinreb on INOVA 400 MHz 9H Singlet 1.33 ppm, 3H Singlet 3.05 ppm, 1H Doublet, J = 7 Hz, 3.35 ppm, 3H Singlet 3.62 ppm, 1H Doublet, J=8 Hz, 3.78 ppm. Measured in $CDCl_3$.

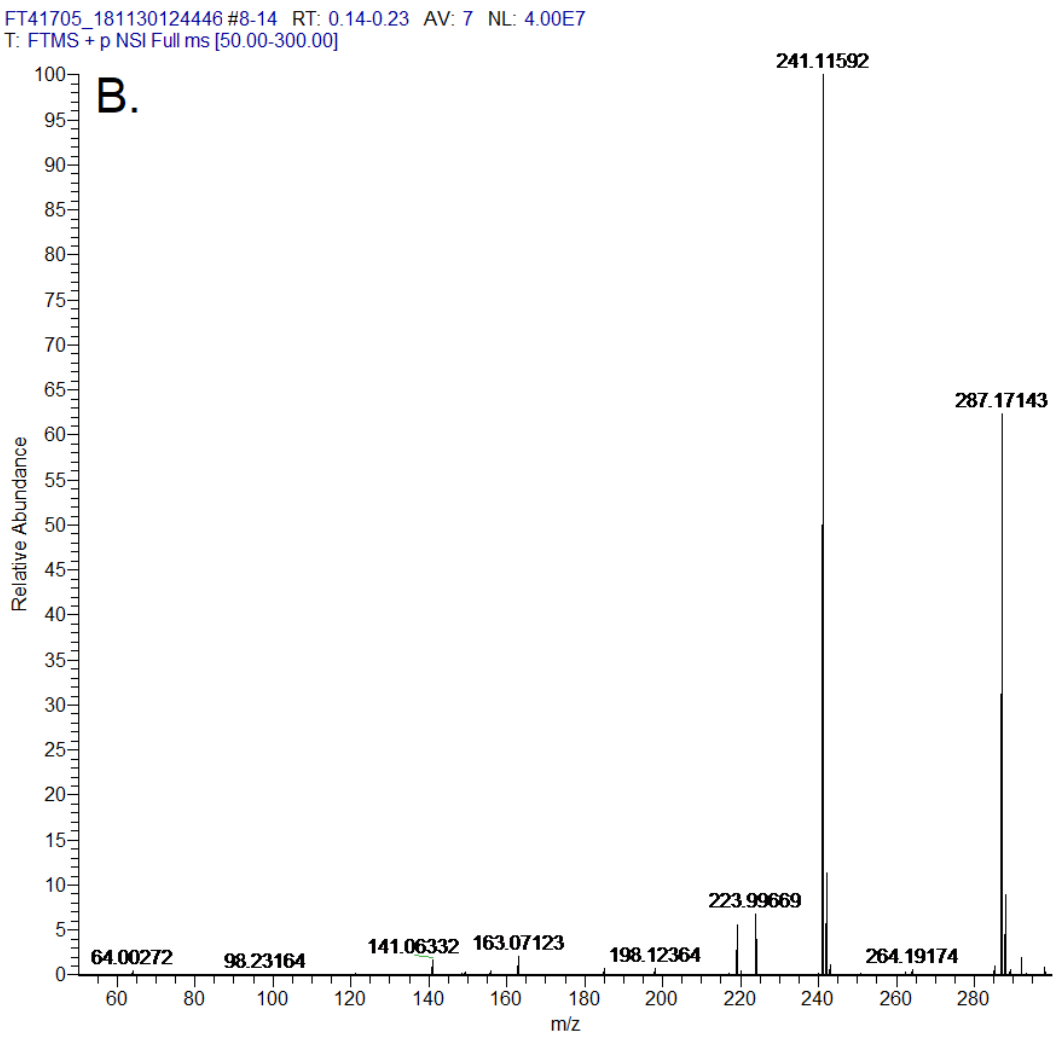

Mass: [Boc G Weinreb + Na] = 241

Figure S2: HCl-NH_2-G-Weinreb

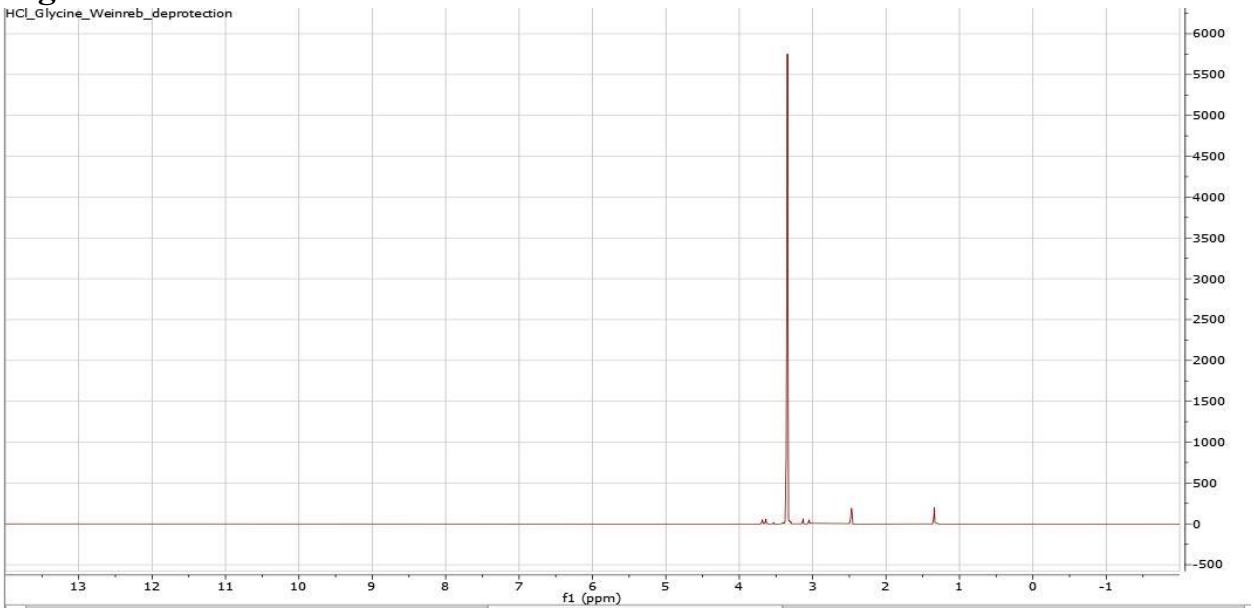

3H Singlet 3.63ppm, 3H Singlet 3.05ppm, 1H d 3.06ppm J=15 Hz, 1H d 3.96ppm J=15 Hz, D_20

Figure S3: Boc-PG-Weinreb NMR and ESI

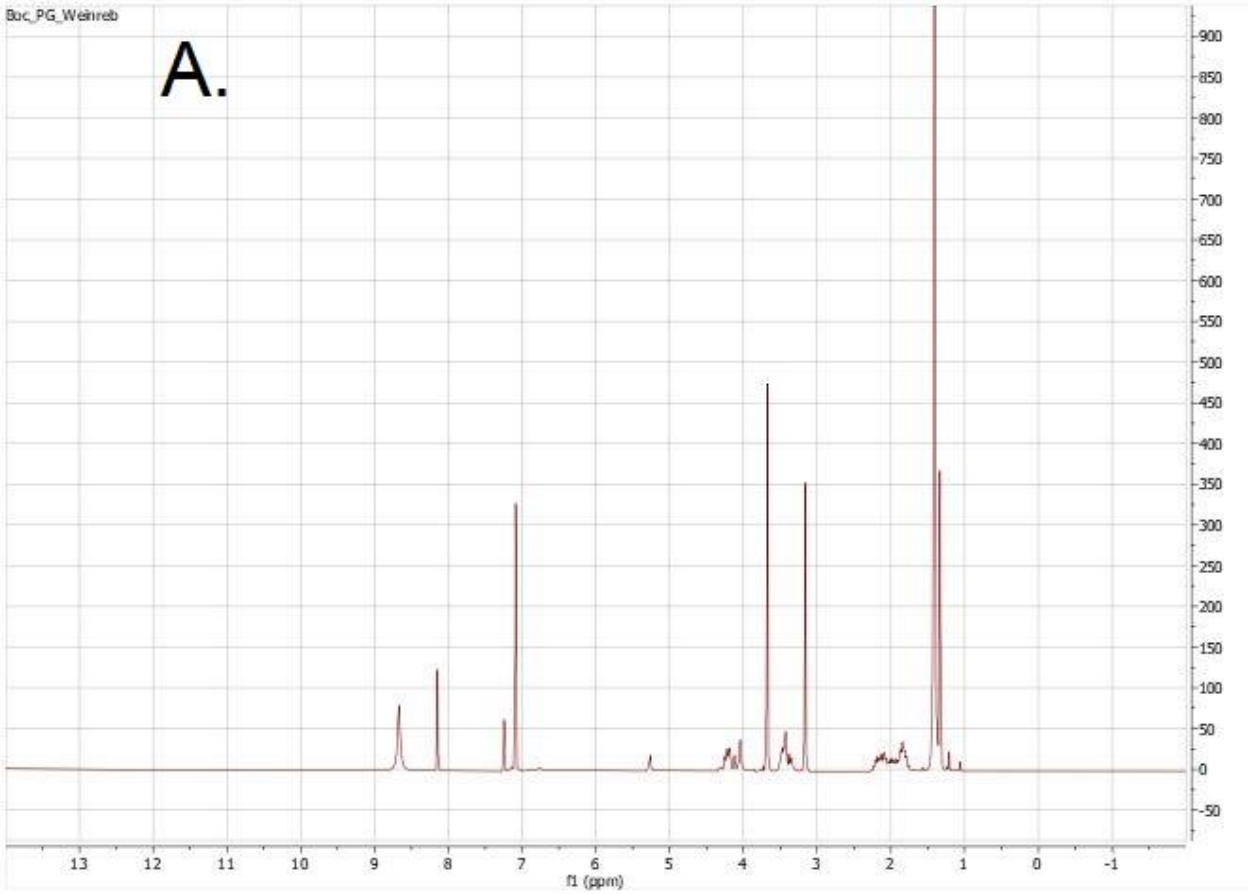

3H Singlet 3.63ppm, 3H Singlet 3.05ppm, 1H d 3.06ppm J=15 Hz, 1H d 3.96ppm J=15 Hz, 2H 1.96 multiplet, 2H 2.28 multiplet, 9H singlet 1.42 ppm, 1H multiplet, 3.69ppm, 1H multiplet 3.57 ppm, $CDCl_3$.

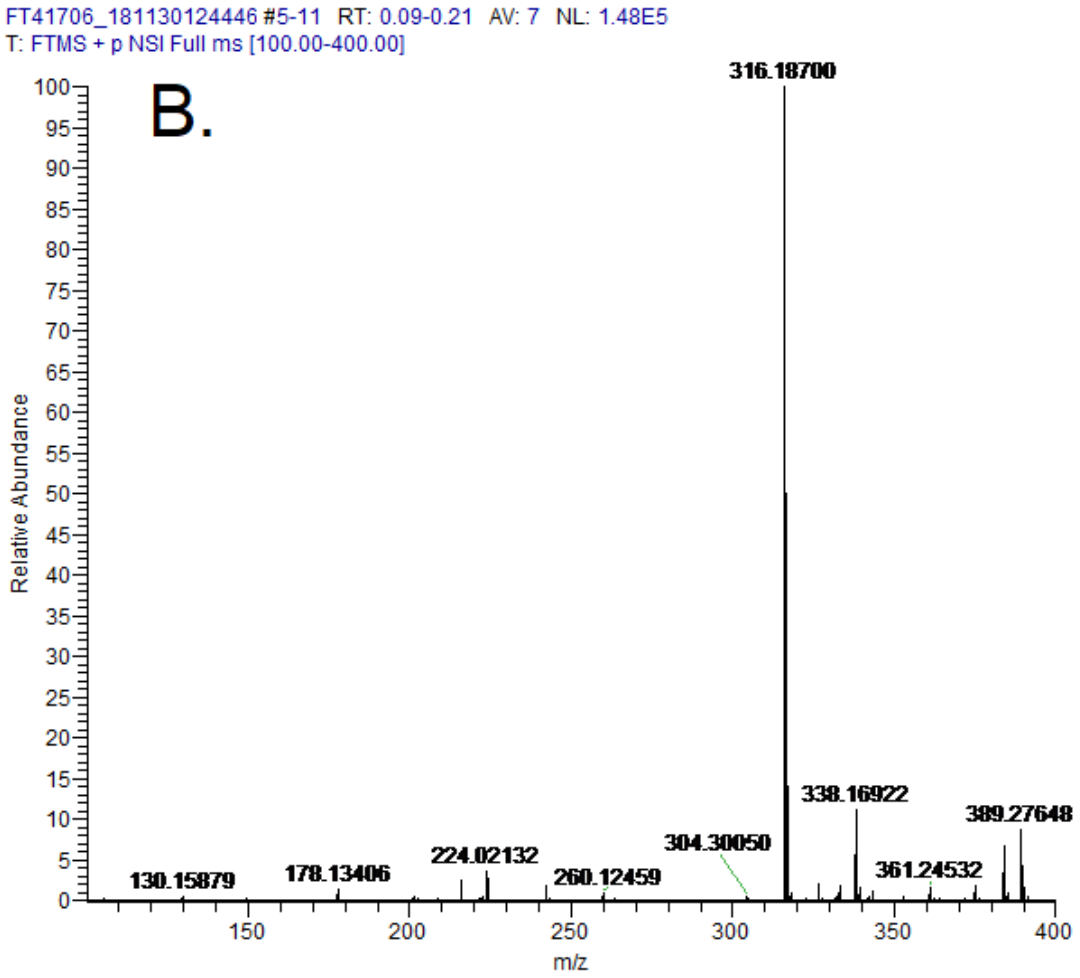

Mass: [Boc PG Weinreb + Na] = 316

Figure S5: HCl-NH_2-PG-Weinreb

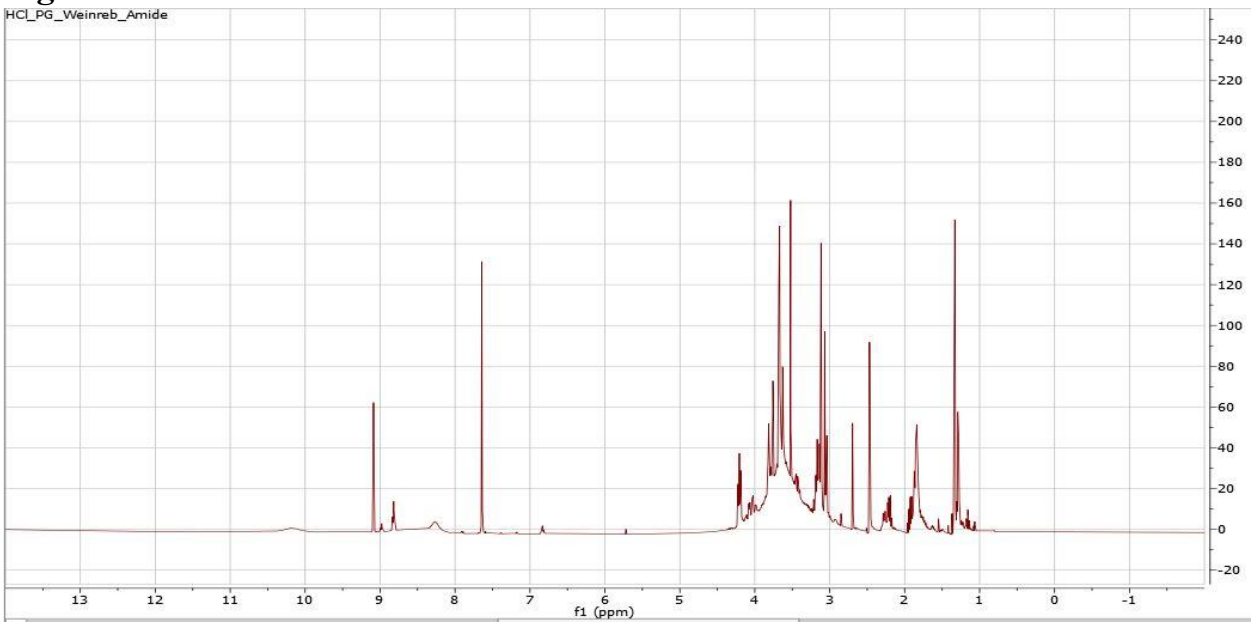

3H Singlet 3.63ppm, 3H Singlet 3.05ppm, 1H d 3.06ppm J=15 Hz, 1H d 3.96ppm J=15 Hz, 2H 1.96 multiplet, 2H 2.28 multiplet, 1H multiplet, 3.69ppm, 1H multiplet 3.57 ppm. D_2O

Figure S6: Fmoc-NPG-Weinreb

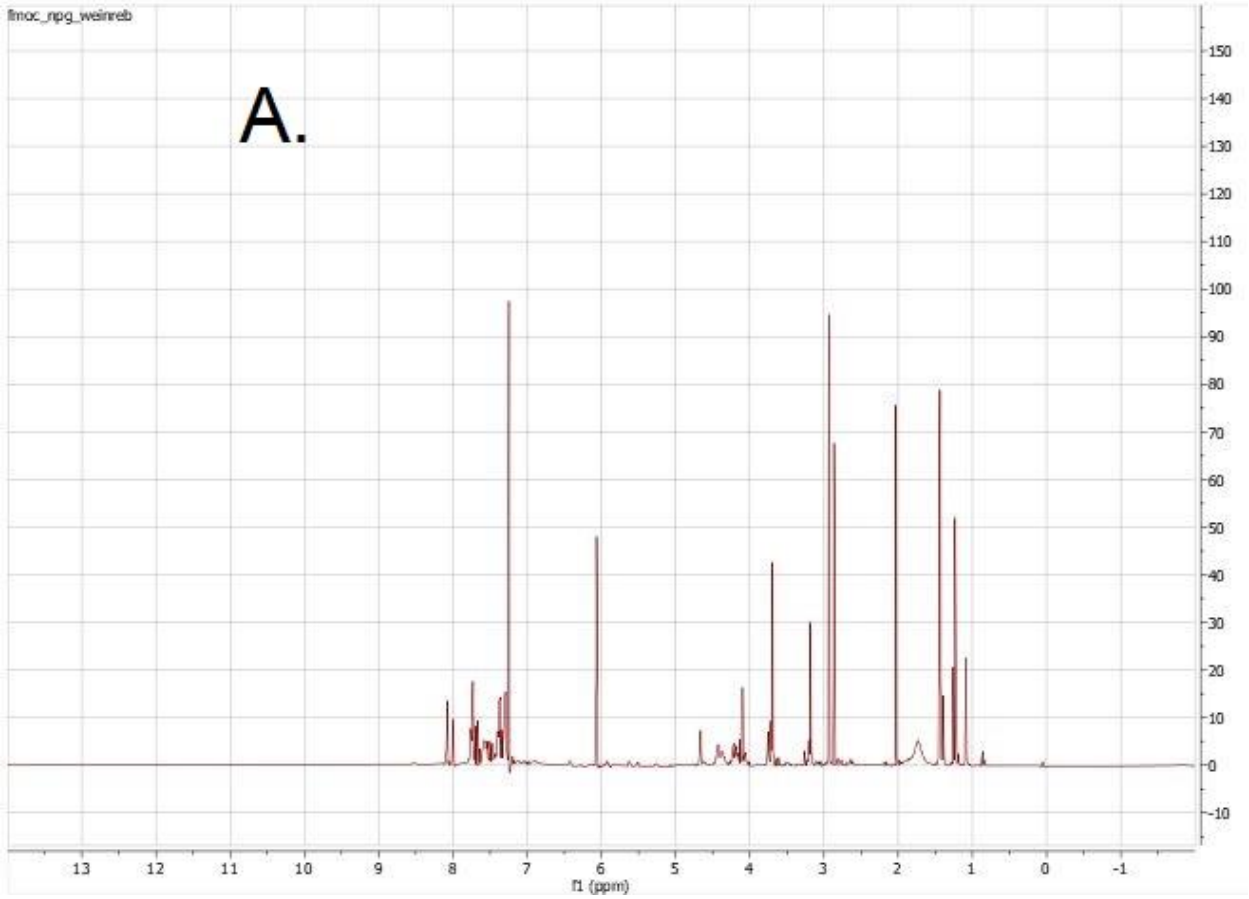

3H Singlet 3.63ppm, 3H Singlet 3.05ppm, 1H singlet 7.24 ppm, 8H multiplet 7.50 ppm, 1H d 3.06ppm J=15 Hz, 1H d 3.96ppm J=15 Hz, 2H 1.96 multiplet, 2H 2.28 multiplet, 1H multiplet, 3.69ppm, 1H multiplet 3.57 ppm, $CDCl_3$

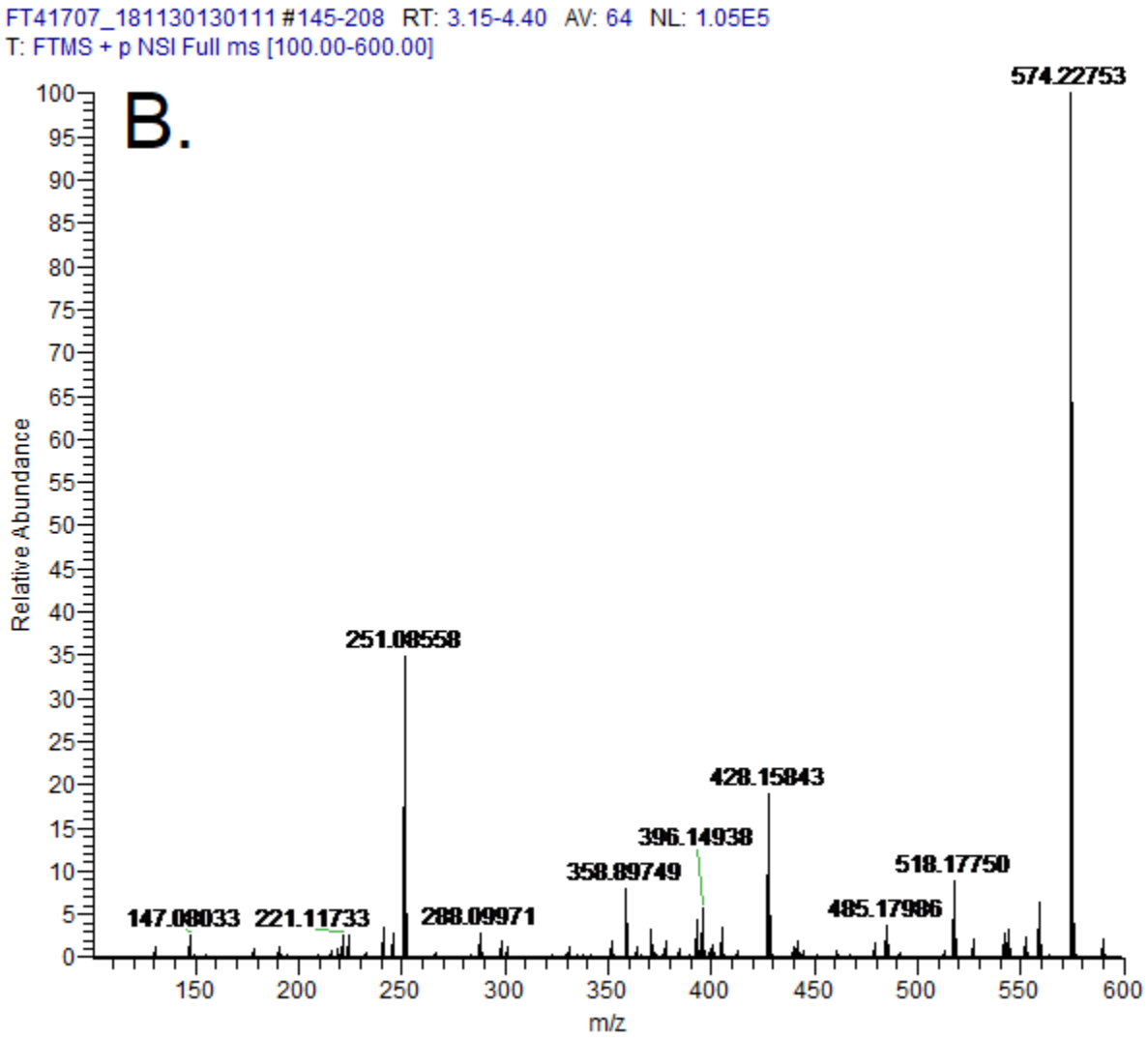

Mass: [Fmoc NPG Weinreb + Na] = 574

Figure S7: Fmoc-NPG-CHO

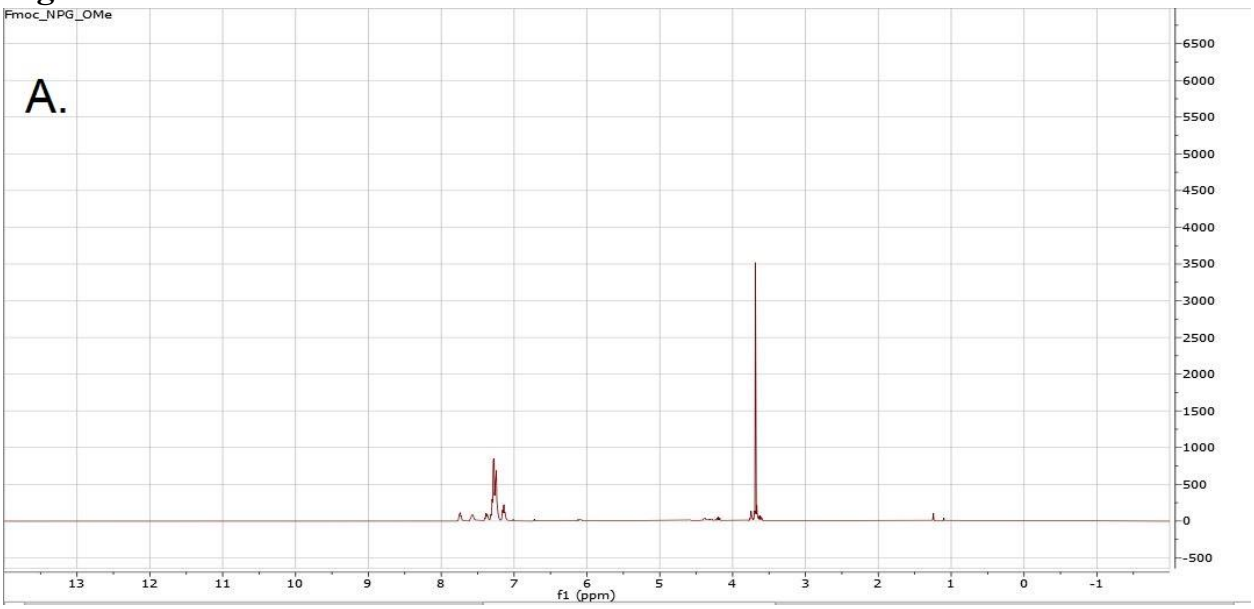

Spectrum of Fmoc NPG CHO did not match the compound, only the LC/MS data was found to match the weight of the theoretical compound. Likely due to a shortcoming in the original procedure used to deprotect the Weinreb amide.

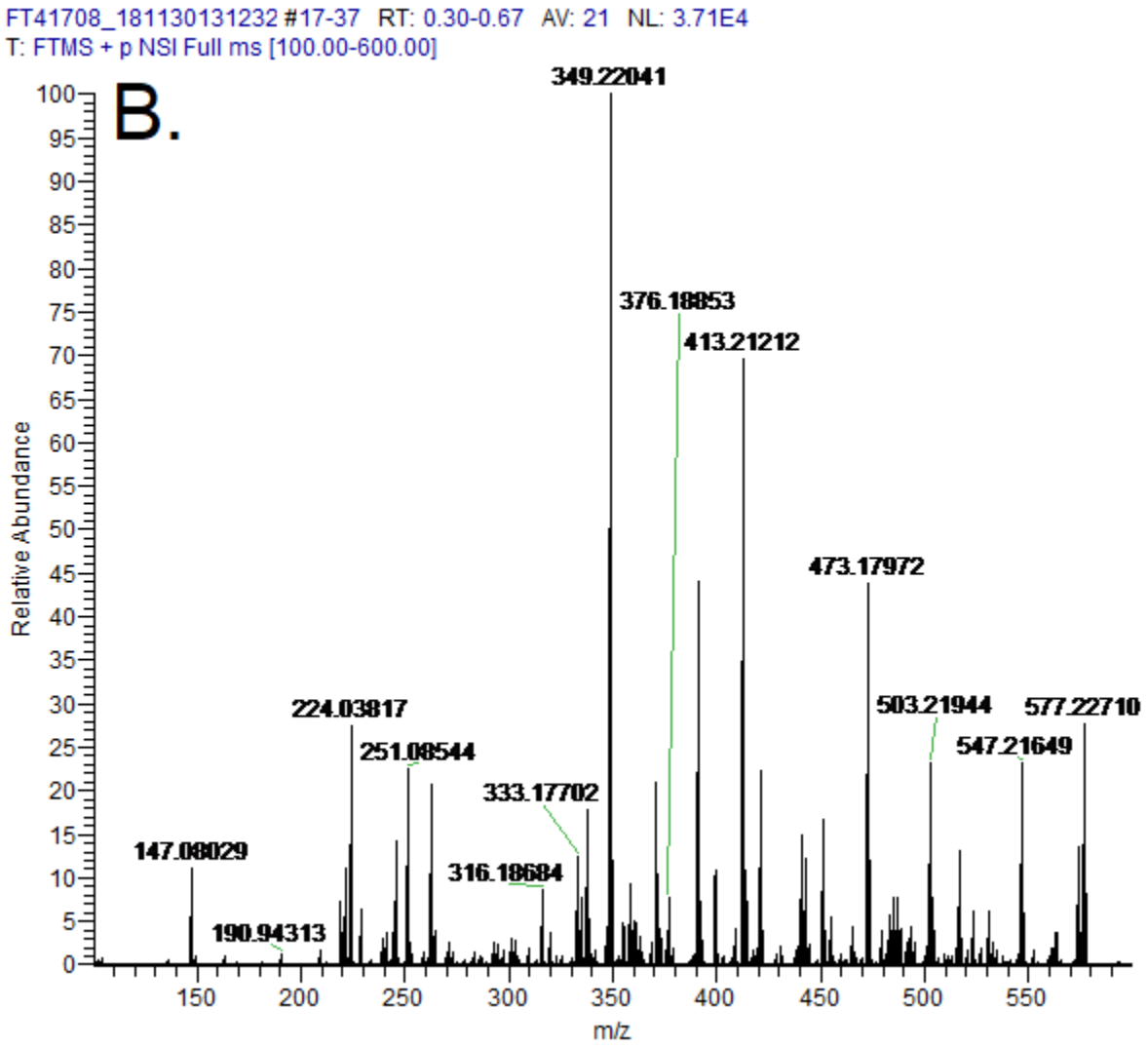

Mass: [Fmoc NPG CHO + Na] = 515

Figure S8: Control NPG

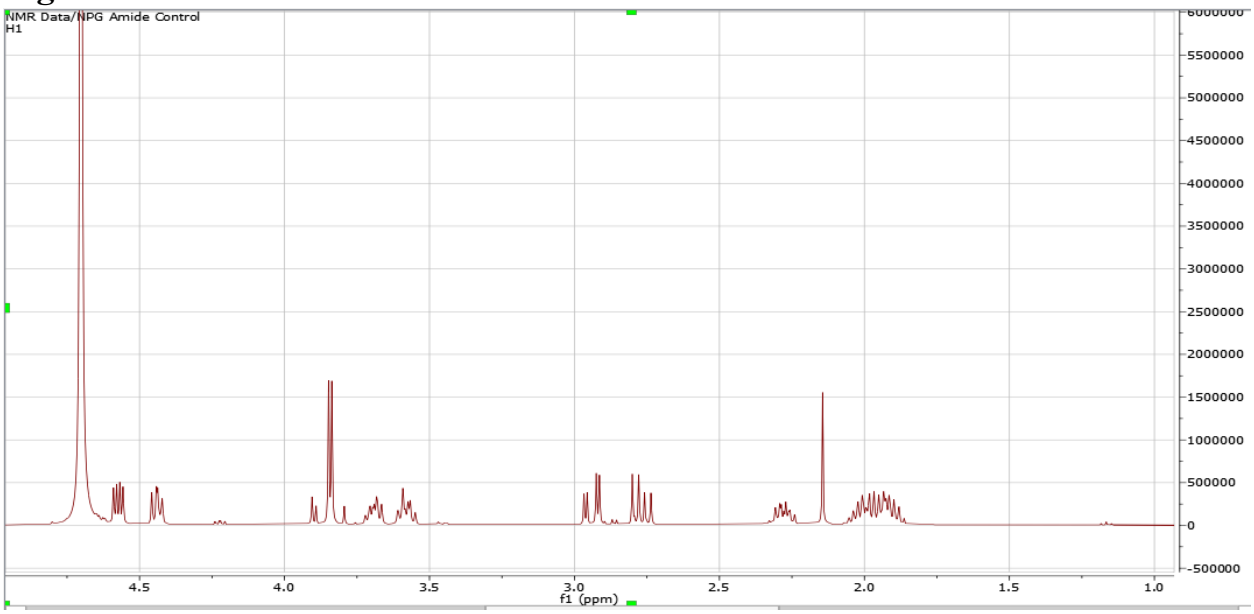

1H d 3.06ppm J=15 Hz, 1H d 3.96ppm J=15 Hz, 2H 1.96 multiplet, 2H 2.28 multiplet, 9H singlet 1.42 ppm, 1H multiplet, 3.69ppm, 1H multiplet 3.57 ppm, 1H 2.76ppm dd j= 15.5 Hz 8.8Hz, 1H 2.93ppm dd j= 15.5 Hz 7.7Hz, D_2O.

Figure S9:10 Equivalents LAH on Control Temperatures

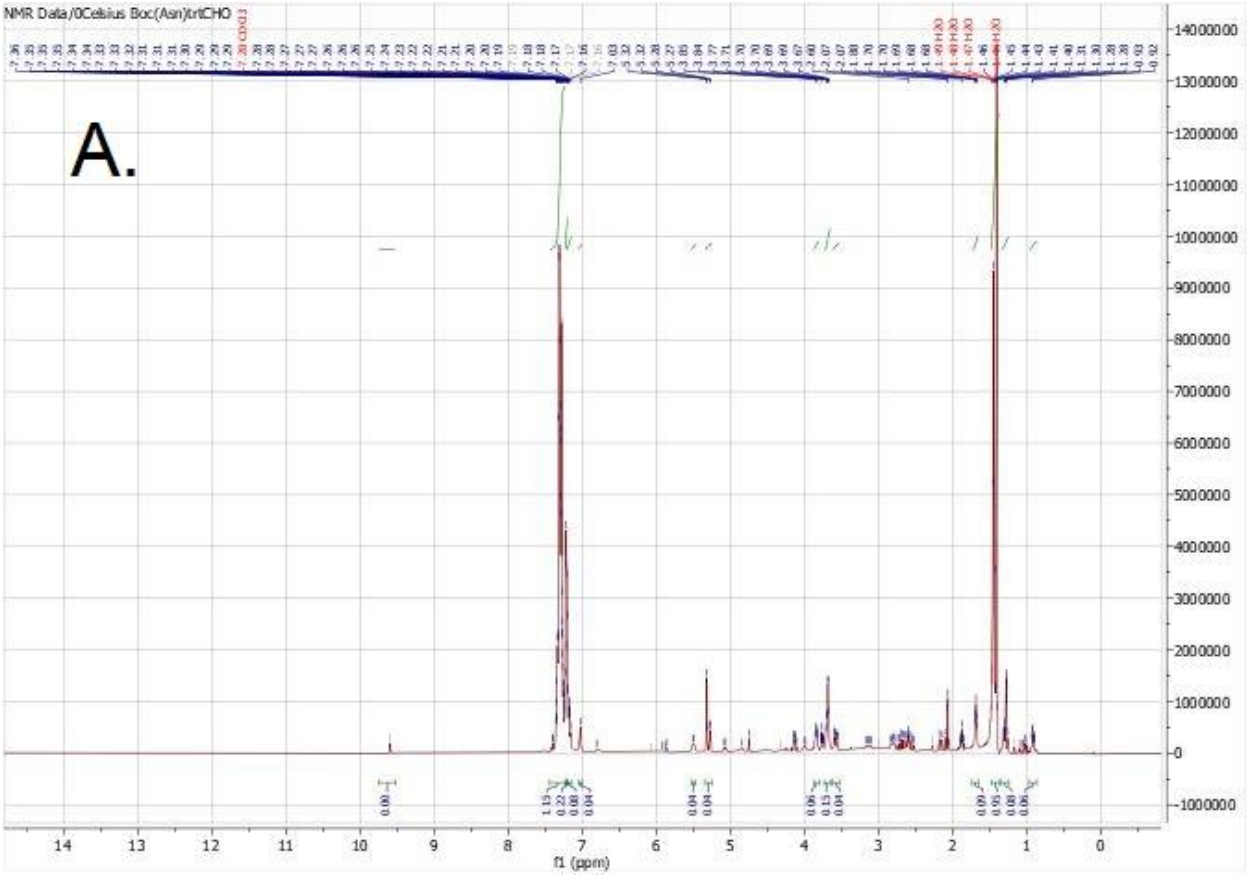

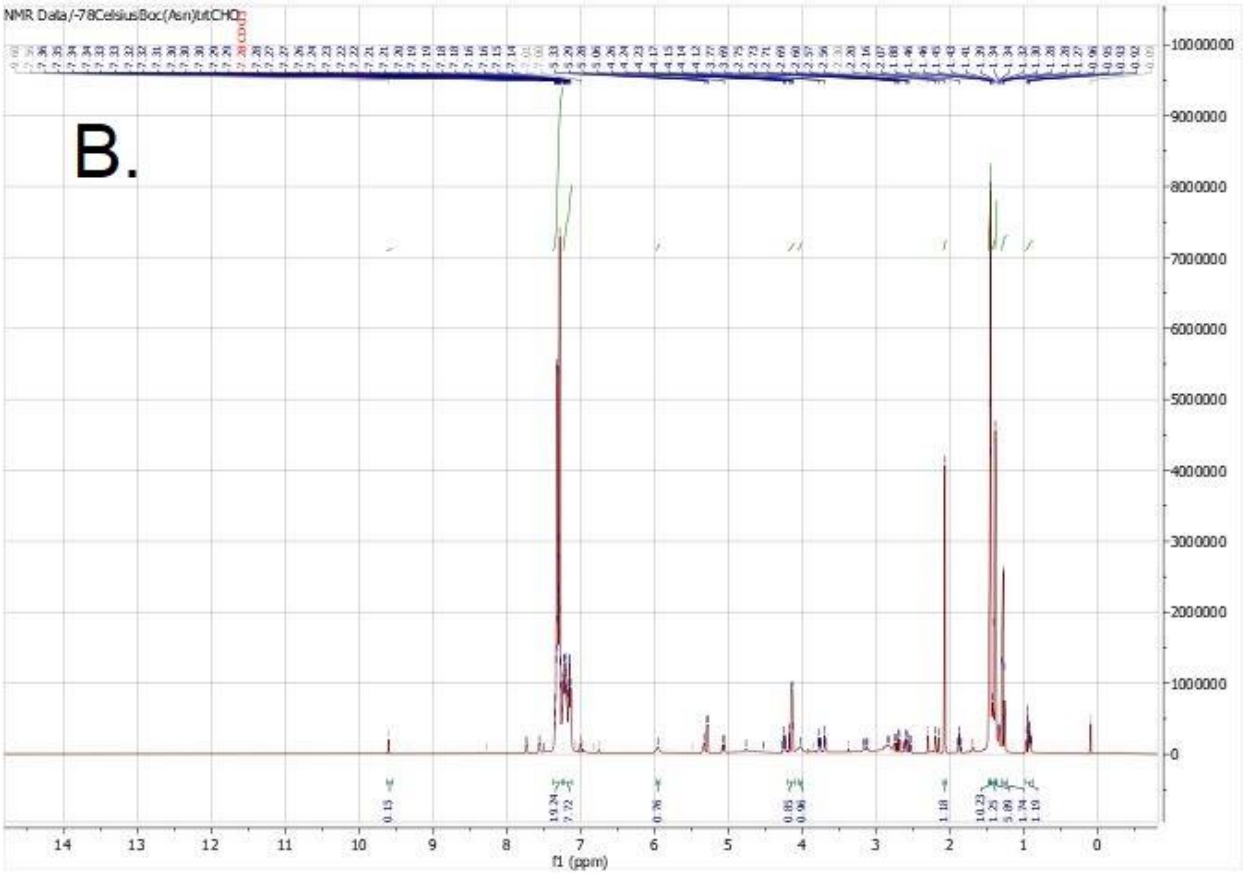

Both spectra were observed for aldehyde peaks at 9.56 and loss of the Weinreb amide at 3.05ppm and 3.63ppm to show full reduction. The -78°C was chosen for the reduction as it was less likely to over reduce the peptide.

Figure S10: 10 Equivalents LAH on Boc trt NPG Resin

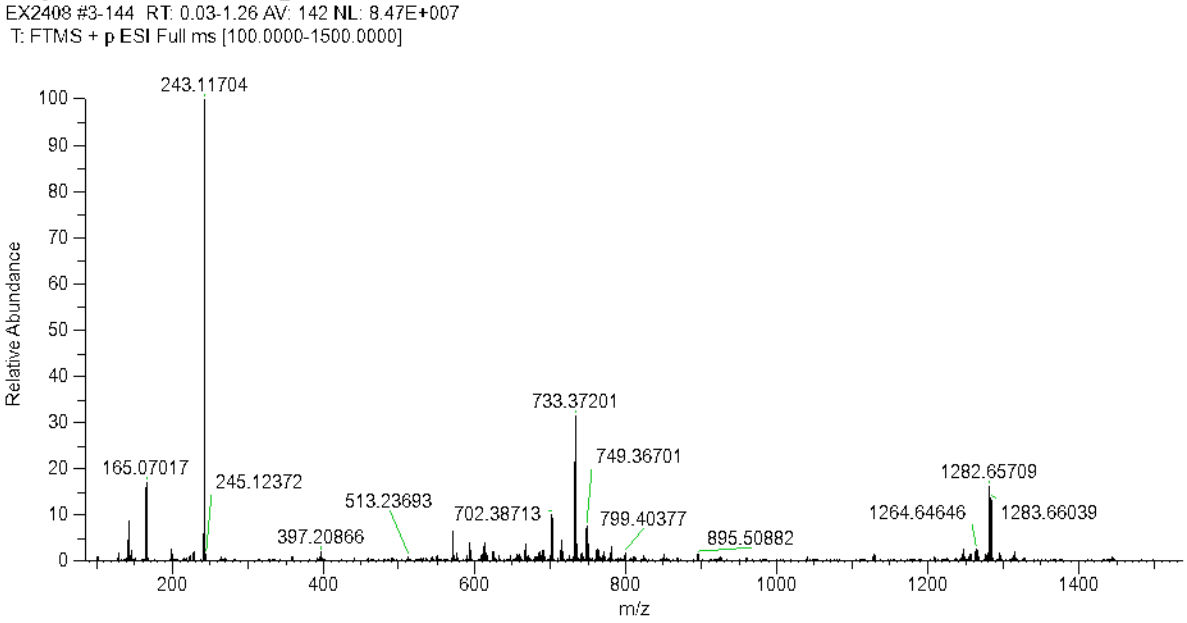

No 612 peak was observed in the spectrum and a number of larger products were observed indicating the compound likely fragmented after treatment with LAH.

Figure S11:1.1 and 2.0 Equivalents LAH on Control

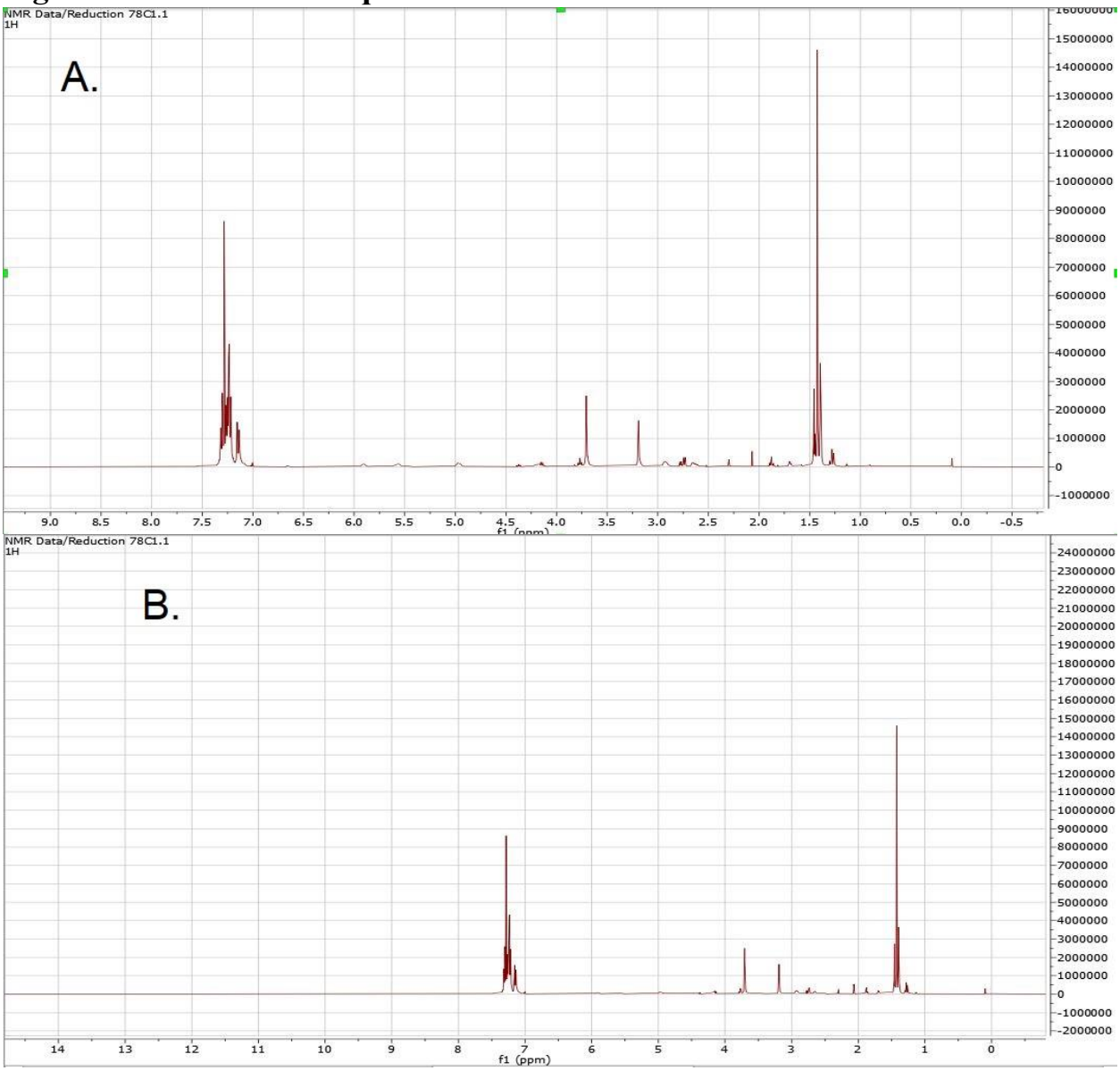

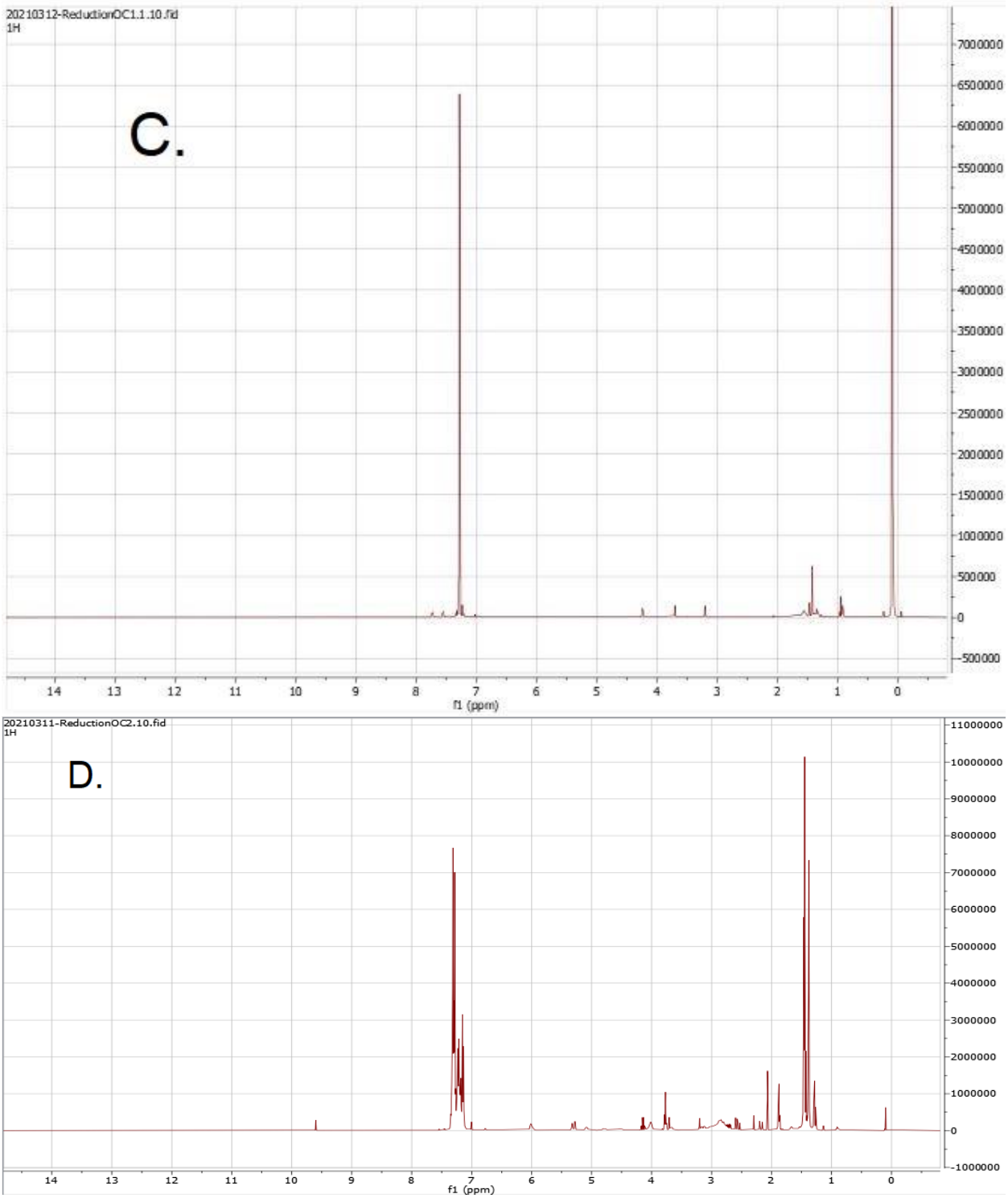

All spectra were analyzed for the 9.56 ppm peak for the aldehyde which was only seen in the 0°C and 2 equivalents of LAH solid. A) is -78°C and 1.1 equivalents, B) is -78°C and 2.0 equivalents, C) is 0°C 1.1 equivalents, D) is 0°C 2.0 equivalents.

Figure S12: 10 Equivalents DIBAL on Boc-trt-NPG Resin

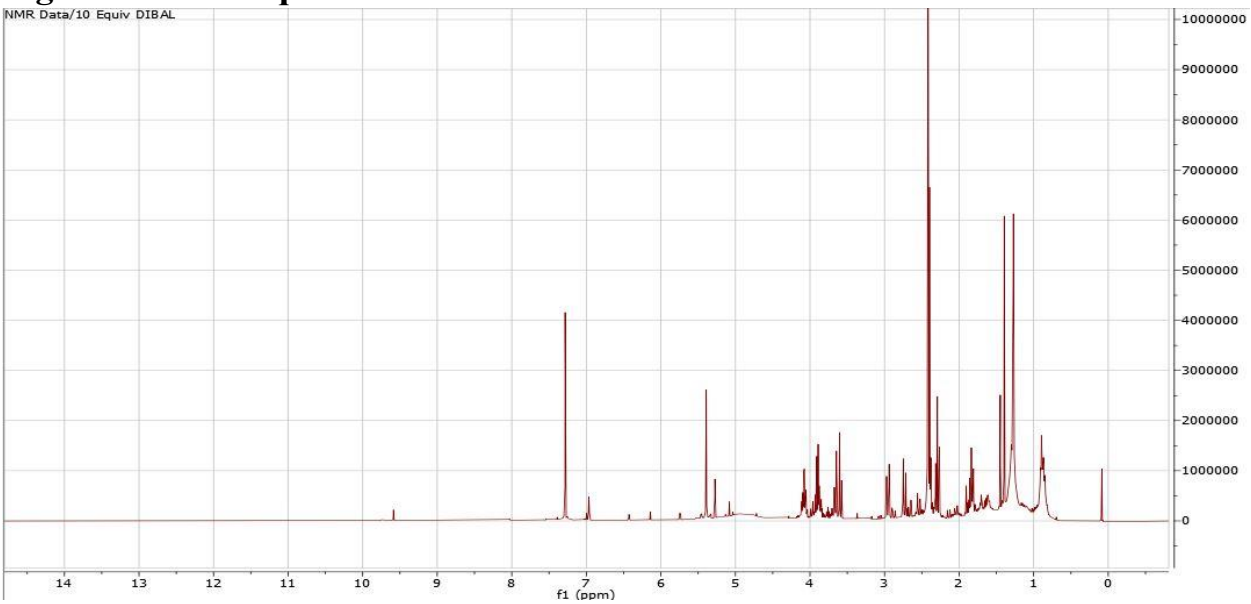

The spectrum was primarily analyzed for the aldehyde peak as it had yet to be purified, the compound was not purified as it would not readily dissolve in acetonitrile.

Figure S13: HPLC and Mass Spec Data for NPG Assembly

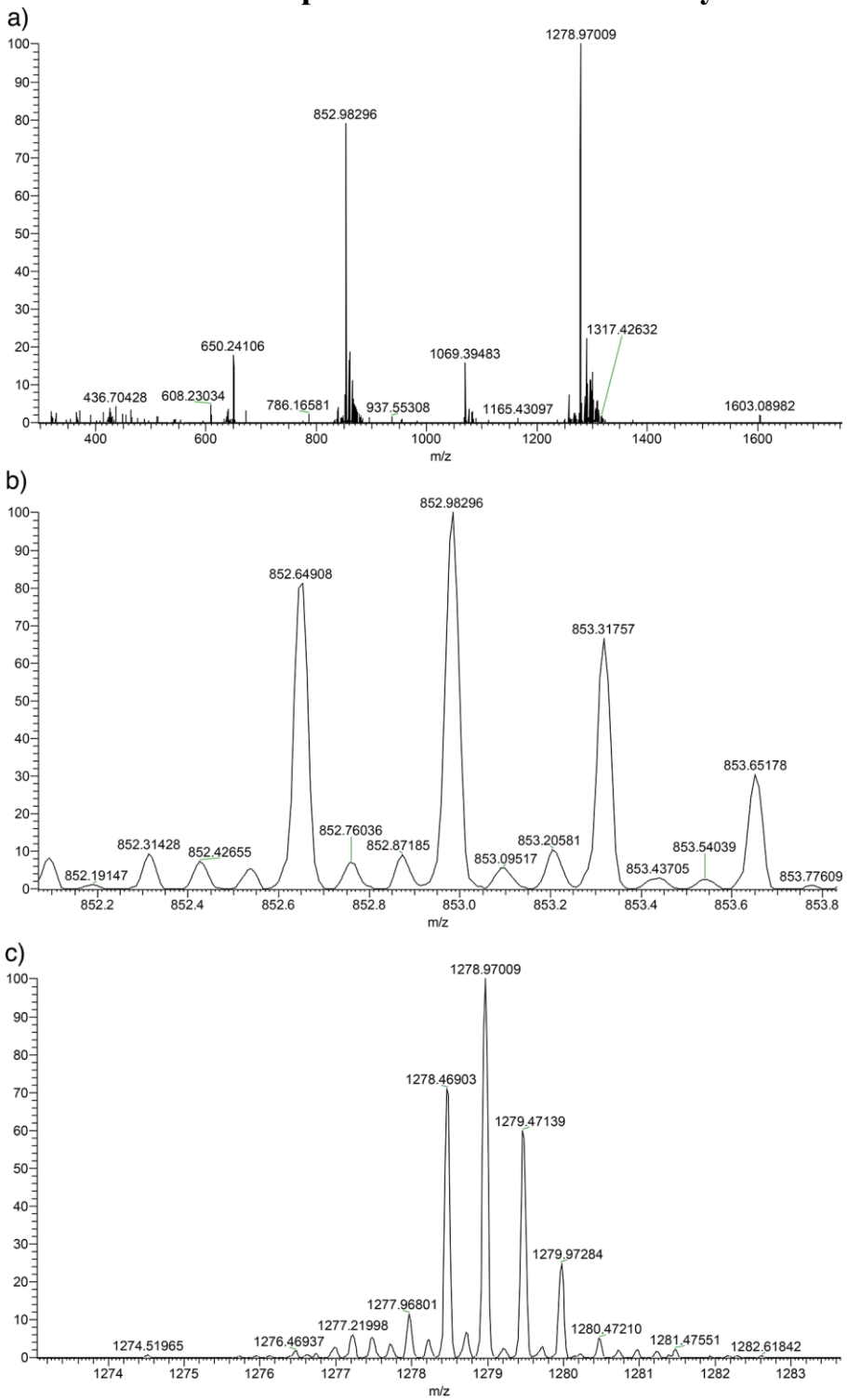

The distances between 852.650, 852.983 and 853.318) are 0.33~0.335 which indicates the charge on the system is +3. Multiplying the mass by 3 gives a mw of 2556 which is in lines with a decamer of NPG in its hydrated form. Distances between peaks 1278.46, 1278.97, and 1279.47 is around 0.5 giving a charge of +2 making the mw also 2556 which is the hydrated decamer structure once again.